DOE/ET-53088-574 IFSR #574

Two-Dimensional Analytic Theory for Toroidal Alfvén Eigenmodes

H. YE, Z. SEDLACEK, and S.M. MAHAJAN
Institute for Fusion Studies
The University of Texas at Austin
Austin, Texas 78712

February 1993

Two-Dimensional Analytic Theory for Toroidal Alfvén Eigenmodes

H. Ye, Z. Sedlacek,[a] and S. M. Mahajan
Institute for Fusion Studies
The University of Texas at Austin
Austin, Texas 78712

Abstract

A two-dimensional analysis of the toroidal Alfvén eigenmodes (TAE) is presented, based on an integrodifferential equation describing the shear Alfvén perturbation of a toroidal plasma equilibrium in terms of coupling among the toroidal Alfvén continua with the usual gap structure. Using a method similar to the Van Kampen-Case analysis for the Vlasov equation, we derive exact analytic expressions for the dispersion function and the two-dimensional eigenmode structure. The dispersion function is expressed in terms of Cauchy-type integrals, which explicitly expresses the global character of TAE modes and facilitates the calculation of their damping. The continuum-damped TAE modes are shown to be, in general, not true eigenmodes of the toroidal plasma equilibrium, but rather resonances corresponding to zeros of the analytic continuation of the dispersion function onto unphysical sheets of its Riemann surface. Approximate but explicit expressions for the dispersion relation and the eigenfunction are also obtained in the limit of vanishing inverse aspect ratio.

[a]Permanent address: Institute of Plasma Physics, Academy of Sciences of the Czech Republic, Prague, Czech Republic

I Introduction

The confinement of high energy, fusion generated alpha particles is crucial for the making of a successful fusion reactor. It has been suspected, for a while, that these energetic particles with steep spatial gradients, and hence a considerable reservoir of free energy, could drive a host of plasma instabilities, some of which could prove harmful to the highly desired alpha particle confinement. Much attention has been recently focused on the interaction of the alpha particles with two kinds of Alfvénic motions, the *global Alfvén eigenmodes*[1–5] (GAE) and the *toroidal Alfvén eigenmodes*[6–8] (TAE), in particular the latter. It was earlier claimed that the TAE could be driven violently unstable,[9] with rather unfortunate consequences. Experiments with high energy beams performed on both TFTR[10] and DIII-D[11] tokamaks, however, indicate that the instability thresholds may be much larger than those predicted by these theories. The clear message was that a much more systematic and detailed calculation of the intrinsic dampings of these modes (in the absence of alpha particles) was called for. In order to meet this challenge, researchers have been investigating a variety of mechanisms. With the exception of a recent paper,[12] which has demonstrated the crucial importance of electron dynamics on toroidal Alfvén waves, most of the studies were conducted within the framework of ideal magnetohydrodynamics (MHD). Two distinct theoretical approaches, based on the variational nature of the determining equations, have been developed to calculate what is generally known as the TAE *continuum damping.*[13–16] Both of these approaches for the continuum damping calculation are effectively one-dimensional, and are valid for high mode numbers and a vanishingly small inverse aspect ratio. In order to go beyond these limiting constraints, we have developed a fully two-dimensional analytic theory for the investigation of TAE modes. Instead of using the usual poloidal harmonic expansion, we decompose the wave function in the natural basis provided by the eigenfunctions of the

toroidal Alfvén continuum. Our method allows us to solve the standard TAE equation analytically for arbitrary inverse aspect ratio (ϵ) and arbitrary mode numbers (n). We must, however, remind the reader that the standard TAE equation itself was derived in the small $\hat{\epsilon}$ limit.

Our paper also addresses a fundamental theoretical question concerning the true nature of the TAE modes. Are they true eigenmodes of the toroidal shear Alfvén wave equation that correspond to zeros of some dispersion function, or are they merely *quasimodes* (such as the Landau-damped modes in a stable plasma) associated with zeros of the *analytic continuation* of the dispersion function onto an unphysical sheet of its Riemann surface? Physical considerations, i.e., that eigenvalues of a conservative system (such as ideal MHD) must necessarily be real or appear in complex-conjugate pairs, lead us to believe that there can be no complex eigenvalues for the MHD system without an alpha particle drive (for instance). Therefore, the continuum-damped TAE modes can not be the true eigenmodes of the system under consideration. They must, in some sense, turn out to be quasimodes. We shall elaborate on this point later in the paper. As a by-product we obtain a systematic method for calculating the eigenfunctions of continuum TAE modes, which play a crucial role in Alfvén-wave and other heating schemes of thermonuclear plasmas.[17]

The contents of this paper are as follows. We begin in Sec. II by recasting the two-dimensional partial differential equation (PDE) for the TAE modes into an integrodifferential equation. This reformulation is analogous to the one used for studying many other basic plasma systems, including the Vlasov equation,[18,19] the equation for electrostatic oscillations in a cold, nonuniform plasma,[20,21] and the MHD equation in a slab geometry.[22,23] The integrodifferential equation is so arranged that, on the left-hand side is an ordinary differential operator describing the toroidal shear Alfvén waves associated with a single flux surface, and on the right-hand side is an integral operator representing the interaction of these waves across the flux surfaces. This reformulation not only brings to light the essential physical

aspects of the TAE system, but may also facilitate our search for the solutions by letting us draw on the recent fascinating developments in the theory of the Vlasov equation.[24–27]

In order to find a more suitable basis than the poloidal harmonics, we analyze in Sec. III the ordinary differential equation (ODE) for the toroidal shear Alfvén waves on a single flux surface. The collection of these waves on all flux surfaces constitutes the toroidal Alfvén continuum.[28–31] For the standard TAE model, this equation can be transformed into the Mathieu equation in the poloidal angle, with radius and frequency appearing as independent parameters. The spectrum of this equation varies continuously with the flux surface and exhibits the familiar gap structure.[32–34,5–7] We also find the continuum eigenfunctions in terms of the Floquet solutions of the Mathieu equation.

In Sec. IV we expand the TAE wave function in terms of the continuum eigenfunctions found in Sec. III, thereby turning the differential operator of the integrodifferential equation into a simple multiplier. The resulting integral equation has many features in common with the Vlasov equation, so we can use the machinery developed for the latter (the *Van Kampen-Case analysis*) to derive analytic expressions for the dispersion function and the eigenfunctions of the discrete TAE modes, and analytic expressions for the eigenfunctions of the continuum TAE modes.

In Sec. V, we simplify the results obtained in Sec. IV in the limit of vanishing inverse aspect ratio. In this limit the integral equation reduces to a finite set of recurrence relations. In the case of a single gap, we solve the dispersion relation and compare it with results previously obtained using the boundary layer analysis.

Finally in Sec. VI we give a few concluding remarks. Most of the detailed calculations of this paper are put into the appendices. In Appendix A we give a derivation for the Green's function of the two-dimensional Laplacian operator. Appendix B contains the calculation of the continuum eigenvalues and eigenfunctions in the small $\hat{\epsilon}$ limit. And in Appendix C we calculate the coefficients of the recurrence relation derived in Sec. V.

II Derivation of the Integrodifferential Equation

In this section we show that the toroidal shear Alfvén system can be cast into an integrodifferential equation of the form

$$\mathcal{D}\psi = \mathcal{L}\psi \ , \tag{1}$$

where ψ denotes the wave function, $\mathcal{D}$ is an ordinary differential operator that describes shear Alfvén waves on a single flux surface, and $\mathcal{L}$ is an integral operator representing the coupling of these waves across flux surfaces (stemming from magnetic shear, density gradient, etc.). The spectrum of $\mathcal{D}$ is a continuous function of the flux surface, and can be identified with the toroidal Alfvén continuum. The interactions embodied by $\mathcal{L}$ can give rise either to the concentration in the continuous spectrum, which is reflected by the existence of the quasimodes, or to true discrete eigenmodes. Integrodifferential equations like (1) are fundamental in plasma physics — three well known examples are (a) the Vlasov equation for warm plasmas, both unmagnetized and magnetized;[18,19] (b) the equation for electrostatic oscillations in cold nonuniform plasmas;[21] and (c) the ideal MHD equation in the slab geometry.[23] Because of its importance, Eq. (1) has been studied extensively and methods for its solution are well-developed.[18,19,2] The main purpose of this paper is to adapt these techniques to analyze and understand the TAE problem.

We begin with the following ideal MHD equation describing the shear Alfvén perturbation in the limit of low plasma beta:

$$\mathbf{b}\cdot\nabla\nabla_\perp{}^2\mathbf{b}\cdot\nabla\delta\phi - \frac{\mathbf{b}\times\nabla(\mathbf{b}\cdot\nabla\delta\phi)}{B}\cdot\nabla\left(\frac{4\pi}{c}J_{||}\right) + \nabla_\perp\cdot\left[\frac{\omega^2}{V_A^2}\nabla_\perp\delta\phi\right] = 0 \ . \tag{2}$$

Here $\delta\phi$ is the perturbed scalar potential, $\mathbf{b}$ and B are, respectively, the directional unit vector and the magnitude of the local equilibrium magnetic field, $J_{||}$ is the equilibrium plasma current parallel to $\mathbf{b}$, V_A is the Alfvén speed, and ω is the mode frequency to be calculated as an eigenvalue. For the present paper we shall restrict ourselves to a large aspect ratio,

axisymmetric tokamak model with circular flux surfaces. In this model, perturbations with different toroidal mode numbers n ($n = 1, 2, 3, \ldots$) are decoupled, and Eq. (2) reduces to the following two-dimensional PDE:

$$\partial_{\|} \nabla_{\perp}{}^2 \partial_{\|} \phi - \frac{1}{r} (r \partial_{\|}'' + 3\partial_{\|}') \partial_{\|} \phi + \nabla_{\perp} \cdot \left[\Omega^2 (1 + 2\hat{\epsilon} \cos\theta) \nabla_{\perp} \phi \right] = 0 \ , \tag{3}$$

where $\phi(r, \theta)$ is the amplitude of $\delta\phi$ for a given n, and

$$\partial_{\|} \equiv -in + \frac{1}{q} \partial_{\theta} \ , \tag{4}$$

with $q(r)$ as the safety factor. In Eq. (3), the primes denote radial derivatives, e.g., $\partial_{\|}' \equiv \partial_r (1/q) \partial_{\theta}$, and

$$\Omega^2(r, \omega) \equiv \frac{R_0^2 \omega^2}{v_a^2(r)} \ , \qquad \hat{\epsilon}(r) \equiv \frac{5r}{2R_0} \ , \tag{5}$$

where R_0 is the major radius of the magnetic axis, $v_a(r) \equiv B_0 / \sqrt{4\pi\rho(r)}$, and $\rho(r)$ is the plasma mass density. Equation (3) is the "standard" model equation for the TAE modes that has been studied in many previous investigations.[7,9,13–16] Since a detailed derivation of Eq. (2) and its transition to Eq. (3) have been given in Ref. 16, we shall not repeat them here.

In order to exhibit that the TAE continuum damping is analogous to the Landau damping in the Vlasov equation, it is necessary to use the perturbed radial electric field $E(r, \theta) \equiv -\partial_r \phi(r, \theta)$ as the wave function. This choice is dictated by the fact that the singularities of $E(r, \theta)$ are of the desired form, i.e., simple poles like $(r - r_c)^{-1}$, which lead to tractable Cauchy-type integrals. We shall impose the following natural boundary conditions on $E(r, \theta)$:

a) $E(r, \theta)$ is periodic in θ,

b) $E(0, \theta)$ is finite,

c) $E(1, \theta) = 0$.

For notational convenience, we have used the normalized radial variable such that $r = 1$ corresponds to the edge of the plasma column. Equation (3), together with the above boundary conditions, poses a well-defined eigenvalue problem, which we will solve without further approximations. Our mathematical procedure allows us to solve Eq. (3) for arbitrary n and $\widehat{\epsilon}$, although the equation itself was derived under the assumption that $\widehat{\epsilon} \ll 1$.

We now proceed to transform Eq. (3) into the promised integrodifferential equation. We multiply Eq. (3) by r^2, then differentiate it with respect to r, and finally divide it by r. After some algebra, which makes use of the relationship

$$\phi(r,\theta) = -\int_0^r dr'\, E(r',\theta) \ , \tag{6}$$

we obtain the following equation:

$$\nabla_\perp{}^2 \left\{ r[\partial_\parallel^2 + g(r,\theta)] E(r,\theta) \right\} = -\frac{1}{r}\left[A(r,\theta,\partial_\theta) E(r,\theta) + B(r,\theta,\partial_\theta) \int_0^r dr'\, E(r',\theta) \right] \ , \tag{7}$$

where

$$g(r,\theta) \equiv \Omega^2 (1 + 2\widehat{\epsilon}\cos\theta) \ , \tag{8}$$

$$A(r,\theta,\partial_\theta) \equiv -2r\partial_\parallel \partial_\parallel' - \left[(\partial_\theta^2 g) + (\partial_\theta g)\partial_\theta \right] \ , \tag{9}$$

and

$$B(r,\theta,\partial_\theta) \equiv \left[(\partial_\parallel^2 + g)\partial_\theta^2 - 2r\partial_\parallel \partial_\parallel' + (\partial_\theta g)\partial_\theta \right]' \ . \tag{10}$$

The two-dimensional Laplacian

$$\nabla_\perp{}^2 \equiv \frac{1}{r}\frac{\partial}{\partial r} r \frac{\partial}{\partial r} + \frac{1}{r^2}\partial_\theta^2 \tag{11}$$

can be inverted using the Green's function method:

$$\nabla_\perp{}^{-2} = \sum_l \int_0^1 dr' r' \int_0^{2\pi} d\theta'\, G_l(r,r') e^{il(\theta-\theta')} \ . \tag{12}$$

In Appendix A, two different but equivalent representations for $G_l(r,r')$ are obtained:

$$G_l(r,r') = -\sum_k \frac{J_l(\xi_{lk}r)J_l(\xi_{lk}r')}{2\pi N_{lk}^2} , \tag{13}$$

and

$$G_l(r,r') = \begin{cases} \dfrac{1}{2\pi} \ln r_> , & l = 0 ; \\ \dfrac{1}{4\pi|l|}\left[(rr')^{|l|} - \left(\dfrac{r_<}{r_>}\right)^{|l|}\right] , & l \neq 0 . \end{cases} \tag{14}$$

Here $J_l(z)$ is the Bessel function of the first kind, ξ_{lk} is its kth zero,

$$N_{lk}^2 \equiv \frac{1}{2}\xi_{lk}^2 J_{l+1}^2(\xi_{lk}) \tag{15}$$

is a normalization constant, $r_< \equiv \min(r,r')$, and $r_> \equiv \max(r,r')$. The first expression (13) is more useful for theoretical development because it is separable, while the second expression (14) is more useful for practical calculation because of its simplicity. Applying Eq. (12) to Eq. (7) we obtain

$$r[\partial_\parallel^2 + g(r,\theta)]E(r,\theta) = -\sum_l \int_0^1 dr' \int_0^{2\pi} d\theta'\, G_l(r,r')e^{il(\theta-\theta')}$$

$$\times \left[A(r',\theta',\partial_{\theta'})E(r',\theta') + B(r',\theta',\partial_{\theta'})\int_0^{r'} dr''\, E(r'',\theta')\right] . \tag{16}$$

Interchanging r', r'' and the order of integrations in the last term, we finally arrive at the desired integrodifferential equation for the TAE modes:

$$[\partial_\parallel^2 + g(r,\theta)]E(r,\theta) = \int_0^1 dr' \int_0^{2\pi} d\theta'\, K(r,\theta;r',\theta',\partial_{\theta'})E(r',\theta') , \tag{17}$$

where the kernel K, an operator in θ, is a continuous function of r and r':

$$K \equiv -\sum_l \frac{e^{il(\theta-\theta')}}{r}\left[G_l(r,r')A(r',\theta',\partial_{\theta'}) + \int_{r'}^1 dr''\, G_l(r,r'')B(r'',\theta',\partial_{\theta'})\right] . \tag{18}$$

Comparing Eqs. (1) and (17) we find the differential operator for the toroidal Alfvén continuum to be

$$\mathcal{D} \equiv \partial_\parallel^2 + g(r,\theta) . \tag{19}$$

Note that $\mathcal{D}$ contains derivatives only in θ; r and ω are merely independent parameters. In the next section we will analyze the spectrum of this operator and calculate its eigenfunctions. These eigenfunctions will provide us with a basis to diagonalize the left-hand side of Eq. (17).

III The Toroidal Alfvén Continuum

The eigenfunctions for the toroidal Alfvén continuum are solutions of the eigenvalue equation

$$\mathcal{D}\psi(r,\theta) \equiv [\partial_{\|}^2 + g(r,\theta)]\psi(r,\theta) = \sigma(r,\omega)\psi(r,\theta) \ , \tag{20}$$

with the boundary condition that $\psi(r,\theta)$ be periodic in θ for all $0 \leq r \leq 1$. This is an ordinary differential equation that can be solved analytically. We will show that, for given ω, the eigenvalues $\sigma(r,\omega)$ are real, continuous functions of r.

Using Eqs. (4) and (8), we can rewrite the continuum equation (20) explicitly as

$$\left[\left(-in + \frac{1}{q}\,\partial_\theta\right)^2 + \Omega^2(1 + 2\hat{\epsilon}\cos\theta)\right]\psi = \sigma\psi \ . \tag{21}$$

By using the inner product definition,

$$\left\langle \psi^\dagger, \psi \right\rangle (r) \equiv \int_0^{2\pi} d\theta\, \psi^\dagger(r,\theta)\psi(r,\theta) \ , \tag{22}$$

it is easy to derive the equation obeyed by the adjoint eigenfunction $\psi^\dagger(r,\theta)$,

$$\left[\left(-in - \frac{1}{q}\,\partial_\theta\right)^2 + \Omega^2(1 + 2\hat{\epsilon}\cos\theta)\right]\psi^\dagger = \sigma\psi^\dagger \ , \tag{23}$$

which is precisely the defining equation for $\psi(r,-\theta)$. Since both $\psi^\dagger(r,\theta)$ and $\psi(r,-\theta)$ satisfy the same boundary condition, we can put $\psi^\dagger(r,\theta) \equiv \psi(r,-\theta)$ without loss of generality. In the rest of the paper, $\psi^\dagger(r,\theta)$ will not appear.

Equation (21) can be transformed into the standard form of the *Mathieu equation* by a simple change of variables,

$$\theta \equiv 2z \ , \qquad \psi \equiv e^{inq\theta}\chi \ , \qquad \lambda \equiv 4q^2(\Omega^2 - \sigma) \ , \qquad b \equiv -\hat{\epsilon}(2q\Omega)^2, \tag{24}$$

with the new eigenfunction $\chi(z)$ obeying

$$\frac{d^2\chi}{dz^2} + (\lambda - 2b\cos 2z)\chi = 0 \ . \tag{25}$$

The boundary condition translates into the requirement that $\chi(z)\exp[i2nqz]$ be periodic in z with a period π. With the standard Floquet solution,

$$\chi(z) = e^{i\nu z}\sum_l u_l e^{i2lz} \ , \tag{26}$$

the periodicity condition is ensured if the Floquet exponent $\nu(r)$ satisfies

$$\nu(r) + 2nq(r) = \text{even integer} \ . \tag{27}$$

Below we discuss some properties of the Mathieu equation that are relevant to the problem at hand.

We begin by asking the question whether there can be more than one eigenfunction corresponding to the same eigenvalue. From the mathematical literature[35] we know that for integral $\nu(r)$, Eq. (25) has only one acceptable Floquet solution (26); the other linearly independent solution is unstable, i.e., it is unbounded as $|z| \to \infty$. We also know that if $\nu(r)$ is not equal to an integer and if $\chi(z)$ is a solution, then $\chi(-z)$ is another solution linearly independent of $\chi(z)$. Therefore, from Eq. (27) it follows that if $2nq$ is an integer, there is only one periodic solution ψ; and if $2nq$ is not an integer, then again there is only one admissible solution ψ since only one of the two linearly independent solutions

$$e^{i(2nq)z}\chi(z) = e^{i(2nq+\nu)z}\sum_l u_l e^{i2lz} \ , \quad e^{i(2nq)z}\chi(-z) = e^{i(2nq-\nu)z}\sum_l u_l e^{-i2lz} \ , \tag{28}$$

can satisfy the periodicity condition. Thus we conclude that all eigenvalues $\sigma(r,\omega)$ of Eq. (21) are nondegenerate.

Next, let us consider the behavior of the eigenvalues as functions of r. Substituting Eq. (26) into the Mathieu equation (25) yields a recurrence relation

$$[\lambda - (\nu + 2l)^2]u_l - b(u_{l-1} + u_{l+1}) = 0 \ . \tag{29}$$

The eigenvalue equation can be obtained by setting the infinite determinant of Eq. (29) to zero. The "dispersion relation" for the Mathieu equation takes the relatively simple form[35]

$$\sin^2\left(\frac{\nu\pi}{2}\right) = \Delta(\lambda, b)\sin^2\left(\frac{\pi\sqrt{\lambda}}{2}\right) , \tag{30}$$

where $\Delta(\lambda, b)$ is *Hill's determinant.* The behavior of the eigenvalue λ and the corresponding eigenfunction, as functions of ν and b, can be graphically illustrated by the *stability diagrams* such as Fig. 1. In Fig. 1, the shaded regions are the "forbidden zones" where the solutions are unstable, while the unshaded regions are the "allowed zones" where the solutions have the Floquet form. Equation (30) has an infinite number of solutions for λ, reflecting the infinite number of allowed zones; it is moreover invariant if we change the value of ν by an even integer. To enumerate all the eigenvalues unambiguously, we need to divide the domain of ν into intervals according to

$$j \leq |\nu_j| \leq j+1, \quad j = 0, 1, 2 \ldots , \tag{31}$$

then for given ν_j and b there is a unique eigenvalue λ_j satisfying

$$\lim_{b\to 0} \lambda_j = \nu_j^2 . \tag{32}$$

In order for $\nu_j(r)$ to satisfy Eq. (27), we need to introduce an integer-valued function $m_j(r)$, defined by

$$\nu_j(r) \equiv 2\left[m_j(r) - nq(r)\right] . \tag{33}$$

It is in general necessary to allow $m_j(r)$ to jump at radii where $2nq(r)$ takes on integral values so as to keep $|\nu_j|$ within the bounds set by Eq. (31). In fact it is not difficult to see that at these radii $\nu_j(r)$ must change signs. But since the eigenvalue λ_j is an even function of ν_j, it would remain continuous. Therefore by Eq. (24), the eigenvalue of Eq. (20) reads

$$\sigma_j(r, \omega) \equiv \Omega^2(r, \omega) - \lambda_j(r)/4q^2(r) , \tag{34}$$

and is also a continuous function of r. The dashed lines in Fig. 1 depicts how the parameters (λ_j, b) typically vary as r increases. It illustrates clearly the appearance of the gap structure in the toroidal Alfvén continuum. Figure 2 is a more conventional way of showing the same gap structure in the r-ω^2 plane, where the curves are the solutions of $\sigma_j(r,\omega) = 0$. Thus, considering ω as the spectral parameter, the differential operator (19) is seen to have a purely continuous real spectrum. The dashed vertical lines in Fig. 2 indicate the location of the gaps, where $2nq(r)$ takes on integral values, and where $m_j(r)$ may be discontinuous.

Finally, we calculate the eigenfunctions of the Mathieu equation by substituting λ_j into the recurrence relation (29) and solving for the Fourier coefficients $u_l^j(r)$. Up to a normalization factor, these coefficients are uniquely determined.[35] This normalization factor in general depends on r, and can be so chosen that the continuum eigenfunction,

$$\psi_j(r,\theta) = e^{im_j(r)\theta} \sum_l u_l^j(r) e^{il\theta} \ , \tag{35}$$

is continuous over all $0 \leq r \leq 1$. In the limit of small b, the $l = 0$ term in the sum is predominant away from the gaps. Near a gap, however, one of the $l = \pm 1$ terms also becomes important. Thus the value of $m_j(r)$ coincides with the usual poloidal harmonic on each segment of the continuum delimited by the dashed vertical lines in Fig. 2, which shows more graphically why $m_j(r)$ needs to be discontinuous at the gaps. Explicit expressions for the continuum eigenvalue $\sigma_j(r,\omega)$ and the continuum eigenfunction $\psi_j(r,\theta)$ in the small b limit are calculated in Appendix B.

For any given radius r, the eigenfunctions $\psi_j(r,\theta)$ form an orthogonal and complete set. The orthogonality condition reads [recall that $\psi^\dagger(r,\theta) = \psi(r,-\theta)$]

$$\int_0^{2\pi} d\theta \, \psi_i(r,-\theta)\psi_j(r,\theta) = 2\pi N_j^2(r)\delta_{ij} \ , \tag{36}$$

where

$$N_j^2(r) \equiv \sum_l \left[u_l^j(r)\right]^2 \ . \tag{37}$$

In the next section we shall return to the integrodifferential equation (17) and expand the wave function $E(r,\theta)$ in terms of $\psi_j(r,\theta)$. This will enable us to diagonalize the differential operator on the left-hand side and pave the path for solving the entire TAE equation explicitly.

IV The Dispersion Relation and Mode Structure

Now let us expand the wave function $E(r,\theta)$ in terms of the complete set of continuum eigenfunctions $\psi_i(r,\theta)$ found in the previous section:

$$E(r,\theta) = \sum_{i=0}^{\infty} c_i(r)\psi_i(r,\theta) \ . \tag{38}$$

This representation diagonalizes the continuum operator (19) (converts it into a simple multiplier) and changes Eq. (17) to:

$$\sigma_i(r,\omega)c_i(r) = \sum_{j=0}^{\infty} \int_0^1 dr' \, K_{ij}(r,r')c_j(r') \ , \tag{39}$$

where

$$K_{ij}(r,r') \equiv \frac{1}{2\pi N_i^2} \int_0^{2\pi} d\theta \int_0^{2\pi} d\theta' \, \psi_i(r,-\theta)K(r,\theta;r',\theta',\partial_{\theta'})\psi_j(r',\theta') \ . \tag{40}$$

Using the continuum eigenfunction (35), and the kernel (18) with the Bessel function representation (13) for $G_l(r,r')$, we obtain

$$K_{ij}(r,r') = \frac{1}{N_i^2(r)} \sum_{l,k} L_{lk}^i(r) R_{lk}^j(r') \ , \tag{41}$$

where

$$L_{lk}^i(r) \equiv \frac{1}{N_{lk} r} J_l(\xi_{lk} r) u_{l-m_i}^i(r) \ , \tag{42}$$

and

$$R_{lk}^j(r) \equiv \frac{1}{N_{lk}} \int_0^{2\pi} \frac{d\theta}{2\pi} \, e^{-il\theta} \left[J_l(\xi_{lk} r) A(r,\theta,\partial_\theta) + \int_r^1 dr' \, J_l(\xi_{lk} r') B(r',\theta,\partial_\theta) \right] \psi_j(r,\theta) \ . \tag{43}$$

The continuity of kernel $K_{ij}(r,r')$ is guaranteed by the continuity of the original kernel (18) and the continuum eigenfunctions $\psi_i(r,\theta)$. It is remarkable that this kernel is separable, i.e., it is a sum of products of the form $a(r)\,b(r')$. This property will enable us to transform the integral equation into an equivalent set of algebraic equations. Generally speaking, the number of algebraic equations thus obtained is infinite, so in practice it must be truncated in order to obtain useful solutions. In this section we concentrate on the general properties of Eq. (39). The appropriate truncation scheme will be discussed in the next section for the limiting case $\widehat{\epsilon} \to 0$.

Equation (39) has the same structure as the Vlasov equation in action-angle variables with the streaming operator diagonalized by means of its eigenfunctions.[18] Below we apply the method developed in Refs. 18 and 19 to analyze the spectrum of Eq. (39).

The Discrete Spectrum

The discrete spectrum occurs when $\sigma_i(r,\omega) \neq 0$ for all i and for the entire range $0 \leq r \leq 1$. We can explicitly exploit this property of $\sigma_i(r,\omega)$ by introducing the following ansatz:

$$c_i(r) \equiv \frac{\Phi_i(r,\omega)}{\sigma_i(r,\omega)} \,, \tag{44}$$

where the functions $\Phi_i(r,\omega)$ describe the "envelope" of the mode structure. Upon substituting it into Eq. (39), we obtain

$$\Phi_i(r,\omega) = \frac{1}{N_i^2(r)} \sum_{l,k} L_{lk}^i(r) \left[\sum_{j=0}^{\infty} \int_0^1 dr' \, \frac{R_{lk}^j(r')}{\sigma_j(r',\omega)} \, \Phi_j(r',\omega) \right] \,. \tag{45}$$

It is obvious that the choice

$$\Phi_i(r,\omega) = \frac{1}{N_i^2(r)} \sum_{l,k} L_{lk}^i(r) C_{lk}(\omega) \,, \tag{46}$$

converts Eq. (45) into an infinite set of homogeneous algebraic equations in the coefficients $C_{lk(\omega)}$ [a knowledge of $C_{lk(\omega)}$ determines $\Phi(r,\omega)$],

$$C_{lk}(\omega) - \sum_{l',k'} \mathcal{M}_{lk,l'k'}(\omega) C_{l'k'}(\omega) = 0 \,, \tag{47}$$

where

$$\mathcal{M}_{lk,l'k'}(\omega) \equiv \sum_{i=0}^{\infty} \int_0^1 dr \, \frac{R^i_{lk}(r) L^i_{l'k'}(r)}{N_i^2(r)\sigma_i(r,\omega)} \tag{48}$$

is a sum of generalized Cauchy-type integrals of the kind treated by Gakhov.[36] Each integral defines a function of ω, analytic in the whole ω plane except for those ω that satisfy the relation $\sigma_i(r,\omega) = 0$. Thus we arrive at an explicit analytic expression for the dispersion relation for discrete TAE modes:

$$D(\omega) \equiv \det |\delta_{ll'}\delta_{kk'} - \mathcal{M}_{lk,l'k'}(\omega)| = 0 \; . \tag{49}$$

If a nontrivial solution C_{lk} of Eq. (47) were to exist, the two-dimensional eigenfunction:

$$E(r,\theta) = \sum_{i=0}^{\infty} \frac{\psi_i(r,\theta)}{N_i^2(r)\sigma_i(r,\omega)} \left[\sum_{l,k} L^i_{lk}(r) C_{lk} \right] \tag{50}$$

could be readily computed.

Now let us consider the circumstances that may give rise to discrete eigenmodes. In a general configuration, the gaps in the toroidal Alfvén continuum do not line up with each other, so for any real ω, there will be some $\sigma_i(r,\omega)$ that vanishes at some radii. As a consequence the entire real ω-axis is a line of singularity of $\mathcal{M}(\omega)$ and, in turn, of $D(\omega)$. More precisely, we should say that the entire real ω-axis is covered by (overlapping) branch cuts of $D(\omega)$, one for each segment of the continuum in Fig. 2, with each end-point of these segments generating a branch point of $D(\omega)$. Therefore the principal sheets of the Riemann surface of $D(\omega)$ are two disjoint half planes. We observe that $D(\omega)$ is real and depends only on ω^2, so the complex zeros of $D(\omega)$ must appear in quadruplets, $\pm\omega$ and $\pm\omega^*$, with two in each of the half planes. Thus, accepting the reasonable assumption that our starting equation (3) has no unstable eigenmodes, we can infer that $D(\omega)$ has no complex zeros on the principal sheets of its Riemann surface. This leads to the conclusion that, in a general configuration, the ideal MHD toroidal Alfvén spectrum does not contain discrete eigenmodes. The exceptional case occurs when all the gaps in Fig. 2 do line up with each other, so there

exists an interval on the real ω axis where $\sigma_i(r,\omega) \neq 0$ for all i and all $0 \leq r \leq 1$. In this case $D(\omega)$ has a principal Riemann sheet that is connected, and it may have real zeros within the gaps.

On the other hand, even if $D(\omega)$ does not have zeros on the principal sheets of its Riemann surface, its analytic continuation through the branch cuts onto the "unphysical" sheets may still have zeros, just as in the case of the Vlasov equation for a stable plasma. These zeros do not correspond to the true eigenmodes of the original equation. They are rather resonances of the continuous spectrum of the system, which are sometimes called *quasimodes*. It is worth noting that the Cauchy-type integral representation in Eq. (48) makes the analytic continuation of the dispersion function $D(\omega)$ explicit and straightforward — we simply need to carry out the r-integral along appropriate Landau contours. Because of the extremely complicated structure of the Riemann surface of $D(\omega)$ due to the overlapping branch cuts, we shall not deal with these quasimodes in this paper.

The Continuous Spectrum

Next we turn to the continuous spectrum, which occurs when ω is real and $\sigma_i(r,\omega)$ vanishes for some i at some radii. For simplicity we restrict ourselves to the situation where $\sigma_i(r,\omega)$ vanishes only at isolated radial locations. Then by the implicit function theorem, $\sigma_i(r,\omega) = 0$ defines some functions $r_{i\alpha}(\omega)$ (usually more than one, so we use the index α to distinguish them) such that

$$\sigma_i(r_{i\alpha}(\omega),\omega) \equiv 0, \qquad \frac{\sigma_i}{r}(r_{i\alpha}(\omega),\omega) \equiv \sigma_i'(r_{i\alpha}(\omega),\omega) \neq 0 \ . \tag{51}$$

Again, we introduce an ansatz for $c_i(r)$ similar to the Van Kampen-Case eigenmodes:[18–21]

$$c_i(r) = \Lambda(\omega) \sum_\alpha \frac{\delta(r - r_{i\alpha})}{\sigma_i'(r_{i\alpha},\omega)} + P\,\frac{\Psi_i(r,\omega)}{\sigma_i(r,\omega)} \ , \tag{52}$$

where the functions $\Lambda(\omega)$ and $\Psi_i(r,\omega)$ are to be determined. Inserting this into Eq. (39) yields

$$\Psi_i(r,\omega) = \frac{1}{N_i^2(r)} \sum_{l,k} L^i_{lk}(r) \left[\Lambda(\omega) \sum_{j,\alpha} \frac{R^j_{lk}(r_{j\alpha})}{\sigma_i'(r_{i\alpha},\omega)} + \sum_{j=0}^{\infty} P \int_0^1 dr' \, \frac{R^j_{lk}(r')}{\sigma_j(r',\omega)} \Psi_j(r',\omega) \right] . \quad (53)$$

It is obvious that the solution may again be assumed in a form similar to Eq. (46):

$$\Psi_i(r,\omega) = \frac{1}{N_i^2(r)} \sum_{l,k} L^i_{lk}(r) \overline{C}_{lk}(\omega) , \quad (54)$$

leading to the following infinite set of inhomogeneous algebraic equations for $\overline{C}_{lk}(\omega)$,

$$\overline{C}_{lk}(\omega) - \sum_{l',k'} \overline{\mathcal{M}}_{lk,l'k'}(\omega) \overline{C}_{l'k'}(\omega) = B_{lk}(\omega) , \quad (55)$$

where

$$\overline{\mathcal{M}}_{lk,l'k'}(\omega) \equiv \sum_{i=0}^{\infty} P \int_0^1 dr \, \frac{R^i_{lk}(r) L^i_{l'k'}(r)}{N_i^2(r) \sigma_i(r,\omega)} , \quad (56)$$

and

$$B_{lk}(\omega) \equiv \Lambda(\omega) \sum_{j,\alpha} \frac{R^j_{lk}(r_{j\alpha})}{\sigma_j'(r_{j\alpha},\omega)} . \quad (57)$$

The set of linear nonhomogeneous equation (55) always has a nontrivial solution. For if the matrix on the left-hand side is nonsingular, then a unique solution exists for a given (nonzero) $\Lambda(\omega)$; if the matrix on the left-hand side is singular, then the corresponding homogeneous equation has nontrivial solutions, and these solutions are acceptable by letting $\Lambda(\omega) = 0$. Therefore we expect the spectrum for this case to be continuous. In reality, one must truncate this infinite set of equations so that, at least formally, it can be solved by Cramer's rule. Assuming that the solvability conditions are satisfied, we have

$$\overline{C}_{l'k'}(\omega) = \frac{\overline{D}_{l'k'}(\omega)}{\overline{D}(\omega)} , \quad (58)$$

where

$$\overline{D}(\omega) \equiv \det \left| \delta_{ll'} \delta_{kk'} - \overline{\mathcal{M}}_{lk,l'k'}(\omega) \right| , \quad (59)$$

and the determinant $\overline{D}_{l'k'}(\omega)$ is obtained from the determinant $\overline{D}(\omega)$ by replacing its $(lk, l'k')$ element by $B_{lk}(\omega)$. Since every element $B_{lk}(\omega)$ is proportional to $\Lambda(\omega)$, we obtain a consistent solution by putting

$$\Lambda(\omega) = \overline{D}(\omega) \ . \tag{60}$$

Then $\overline{C}_{lk}(\omega)$ and, in turn, $\Psi_i(r,\omega)$, are completely determined.

Alternatively, we can define the eigenfunction for the continuum TAE modes not by means of the principal value as in Eq. (52), but as boundary values on the real axis of the ω plane from above or from below:[18,19]

$$c_j^{\pm}(r) = \Lambda^{\pm}(\omega) \sum_{\alpha} \frac{\delta(r - r_{j\alpha})}{\sigma_j'(r_{j\alpha},\omega)} + P \frac{\Psi_j(r,\omega)}{\sigma_j(r,\omega \pm i0)} \ . \tag{61}$$

Proceeding as before, we find

$$\Lambda^{\pm}(\omega) = D(\omega \pm i0) \ . \tag{62}$$

The functions $\Lambda^{\pm}(\omega)$ are thus equal to the boundary values of the dispersion function $D(\omega)$ on the real axis. This is another manifestation of a general relation that has been found previously in Refs. 18, 20, 21. A detailed discussion and explanation can be found in Ref. 20. By means of the Plemeij formulas it is not difficult to show that the eigenfunctions (52) and (61) are equivalent.

Before closing this section, we remark that, as ω varies, two different roots $r_{j\alpha}(\omega)$ and $r_{j\beta}(\omega)$ may coalesce and disappear. The points of coalescence are always located at the gap radii. At such a point we expect the coefficients $c_j(r)$ for continuum TAE modes to have a term proportional to the δ-function derivative. We note that the ansatz (52) in fact meets this expectation, for as $r_{j\alpha}(\omega)$ and $r_{j\beta}(\omega)$ approach the point of coalescence from opposite sides, the denominators $\sigma_j'(r_{j\alpha},\omega)$ and $\sigma_j'(r_{j\beta},\omega)$ become equal in magnitude and opposite in sign, so the two δ-functions will subtract and produce a term proportional to the δ-function derivative. This property renders the restriction (51) nonessential.

V The Limiting Case $\hat{\epsilon} \to 0$

Until now, our calculation of the solution of the standard TAE equation (3) is rigorous and without any approximations. In particular we have not assumed $\hat{\epsilon}$ to be small. The expressions for the dispersion function (49) and the mode structure (50) and (52) are the exact solution of the mathematical problem represented by Eq. (3). In this section we consider the limiting case $\hat{\epsilon} \to 0$, for which our formalism can be greatly simplified. We shall concentrate on the discrete TAE modes; the calculations for the continuum TAE modes are very similar.

When terms proportional to $\hat{\epsilon} \ll 1$ are neglected, the coefficients A and B [from Eqs. (9) and (10)] become independent of θ:

$$A(r, \partial_\theta) \approx -2r\partial_\parallel \partial'_\parallel \ , \tag{63}$$

$$B(r, \partial_\theta) \approx \left[(\partial_\parallel^2 + \Omega^2)\partial_\theta^2 - 2r\partial_\parallel \partial'_\parallel\right]' \ . \tag{64}$$

Inserting these into Eq. (43) we obtain

$$R^j_{lk}(r) \approx \frac{1}{N_{lk}} \left[J_l(\xi_{lk}r)A_l(r) + \int_r^1 dr'\, J_l(\xi_{lk}r')B_l(r')\right] u^j_{l-m_j}(r) \ , \tag{65}$$

where $A_l(r) \equiv A(r, il)$, and $B_l(r) \equiv B(r, il)$. With the definitions

$$\widehat{L}_{lk}(r) \equiv \frac{J_l(\xi_{lk}r)}{N_{lk}r} \ , \tag{66}$$

$$\widehat{R}_{lk}(r) \equiv \frac{1}{N_{lk}} \left[J_l(\xi_{lk}r)A_l(r) + \int_r^1 dr'\, J_l(\xi_{lk}r')B_l(r')\right] \ , \tag{67}$$

Eq. (48) can be written as

$$\mathcal{M}^{\pm}_{lk,l'k'}(\omega) = \int_0^1 dr\, \widehat{R}_{lk}(r)\widehat{L}_{l'k'}(r) \left[\sum_{j=0}^{\infty} \frac{u^j_{l-m_j}(r)u^j_{l'-m_j}(r)}{N_j^2(r)\sigma_j(r,\omega)}\right] \ . \tag{68}$$

The expression (68), although considerably simpler than the original, still contains an infinite sum. To make further progress, we restrict ourselves to frequencies near the gaps

between the two lowest continua. We will then need to keep only two terms ($j = 0, 1$) in the j-sum, since σ_0, σ_1 alone are $\sim \mathcal{O}(\widehat{\epsilon})$ near the gaps, while all other σ_js tend to be larger (the latter actually increases as j^2 for $j \to \infty$, which ensures the convergence of the series). Furthermore, as $1/\sigma_0$ and $1/\sigma_1$ are highly peaked around the gaps, the main contribution to the integral in Eq. (68) comes from the gap regions. Assuming that the functions $\widehat{L}_{lk}$ and $\widehat{R}_{lk}$ are slowly varying, we can pull them out of the integral and obtain

$$\mathcal{M}_{lk,l'k'}(\omega) \approx \sum_m \widehat{R}_{lk}(r_m)\widehat{L}_{l'k'}(r_m)H_{ll'}(r_m) \ , \tag{69}$$

where m labels the gap located at r_m, which is determined by

$$q(r_m) = q_m \equiv \frac{m + 1/2}{n} \ , \tag{70}$$

and

$$H_{ll'}(r_m) \equiv \sum_{j=0}^{1} \int dx \, \frac{u^j_{l-m_i} u^j_{l'-m_j}}{N_j^2 \sigma_j}(r_m + x) \ , \tag{71}$$

with $x \equiv r - r_m$ measuring the distance from the gap m. Explicit expression for $H_{ll'}(r_m)$ are given in Appendix C, where we find $H_{ll'}(r_m)$ to be a "tridiagonal" matrix whose only significant components are for $l, l' = m, m+1$ [see Eq. (C.4)].

On substituting the simplified expression for $\mathcal{M}_{lk,l'k'}$ [Eq. (69)] into Eq. (47), we obtain

$$C_{lk} = \sum_{m,l'} \widehat{R}_{lk}(r_m)H_{ll'}(r_m)V_{l'}(r_m) \ , \tag{72}$$

where

$$V_l(r_m) \equiv \sum_k \widehat{L}_{lk}(r_m)C_{lk} \ . \tag{73}$$

Combining Eqs. (72) and (73) we can reduce the k index, and obtain a reduced set of algebraic equations:

$$V_l(r_m) = \sum_{m',l'} H_{ll'}(r_{m'})F_l(r_m, r_{m'})V_{l'}(r_{m'}) \ , \tag{74}$$

where

$$F_l(r_m, r_{m'}) \equiv \sum_k \widehat{L}_{lk}(r_m)\widehat{R}_{lk}(r_{m'}) \tag{75}$$

is explicitly separable. Making use of Eq. (C.4), Eq. (74) becomes

$$V_l(r_m) = \alpha_l F_l(r_m, r_l) V_l(r_l) + \alpha_{l-1} F_l(r_m, r_{l-1}) V_l(r_{l-1})$$

$$+ \beta_{l-1} F_l(r_m, r_{l-1}) V_{l-1}(r_{l-1}) + \beta_l F_l(r_m, r_l) V_{l+1}(r_l) \ . \tag{76}$$

With the definition $X_l \equiv V_l(r_l)$, $Y_l \equiv V_{l+1}(r_l)$, the closed subsystem $m = l, l-1$ leads to the following recurrence relation:

$$\begin{pmatrix} 1 - \alpha_l F_l(r_l, r_l) & -\beta_l F_l(r_l, r_l) \\ -\alpha_l F_l(r_{l-1}, r_l) & -\beta_l F_l(r_{l-1}, r_l) \end{pmatrix} \begin{pmatrix} X_l \\ Y_l \end{pmatrix}$$

$$= \begin{pmatrix} \beta_{l-1} F_l(r_l, r_{l-1}) & \alpha_{l-1} F_l(r_l, r_{l-1}) \\ \beta_{l-1} F_l(r_{l-1}, r_{l-1}) & \alpha_{l-1} F_l(r_{l-1}, r_{l-1}) - 1 \end{pmatrix} \begin{pmatrix} X_{l-1} \\ Y_{l-1} \end{pmatrix} \ . \tag{77}$$

Let s and t denote the radially inner- and outermost gaps, respectively, then all quantities to be evaluated at r_l with gap index $l \leq s-1$ or $l \geq t+1$ must vanish, so we have

$$\begin{aligned} [1 - \alpha_s F_s(r_s, r_s)] X_s - [\beta_s F_s(r_s, r_s)] Y_s = 0 \ , \\ -[\beta_t F_{t+1}(r_t, r_t)] X_t + [1 - \alpha_t F_{t+1}(r_t, r_t)] Y_t = 0 \ . \end{aligned} \tag{78}$$

This equation, together with Eq. (77) which relates (X_s, Y_s) to (X_t, Y_t), provides the dispersion equations to be solved. The two-dimensional eigenfunction for the discrete TAE modes, Eq. (50), also simplifies and can be expressed in terms of X_l and Y_l directly. Substituting Eq. (72) into Eq. (50) we obtain

$$E(r, \theta) = \sum_{ll'} e^{il'\theta} Q_l(r) \left[\sum_{j=0}^{1} \frac{u^j_{l'-m_j}(r) u^j_{l-m_j}(r)}{N_j^2(r) \sigma_j(r, \omega)} \right] \ , \tag{79}$$

where

$$Q_l(r) \equiv (\alpha_l X_l + \beta_l Y_l) F_l(r, r_l) + (\alpha_{l-1} Y_{l-1} + \beta_{l-1} X_{l-1}) F_l(r, r_{l-1}) \ . \tag{80}$$

In the case of a single gap m, we have $s = t = m$, so Eq. (78) becomes

$$\begin{aligned} [1 - \alpha_m F_m(r_m, r_m)] X_m - [\beta_m F_m(r_m, r_m)] Y_m = 0 \ , \\ -[\beta_m F_{m+1}(r_m, r_m)] X_m + [1 - \alpha_m F_{m+1}(r_m, r_m)] Y_m = 0 \ . \end{aligned} \tag{81}$$

Setting the determinant of Eq. (81) to zero, and using Eq. (C.7) for α_m and β_m, we obtain an expression which gives the real frequency shift g_m (defined in Appendix B):

$$\frac{-g_m}{\sqrt{1-g_m^2}} = \frac{nq'_m}{\pi q_m^2}\left[\frac{1-(\pi q_m^2/nq'_m)^2 F_m(r_m,r_m)F_{m+1}(r_m,r_m)}{F_m(r_m,r_m)+F_{m+1}(r_m,r_m)}\right] . \tag{82}$$

This expression is very similar to that obtained previously using boundary layer analysis.[7,37]

Finally, we can actually sum the series in Eq. (75) and obtain a simple expression for $F_l(r_m, r_{m'})$. Using Eqs. (66) and (67) we have

$$F_l(r_m,r_{m'}) = \frac{1}{r_m}\left[A_l(r_{m'})\sum_k \frac{J_l(\xi_{lk}r_m)J_l(\xi_{lk}r_{m'})}{N_{lk}^2} + \int_{r_{m'}}^1 dr'\, B_l(r')\sum_k \frac{J_l(\xi_{lk}r_m)J_l(\xi_{lk}r')}{N_{lk}^2}\right] . \tag{83}$$

The summation of the Bessel function series can be carried out using the identity (for $l \neq 0$)

$$\sum_k \frac{J_l(\xi_{lk}r)J_l(\xi_{lk}r')}{N_{lk}^2} = \frac{1}{2|l|}\left[\left(\frac{r_<}{r_>}\right)^{|l|} - (rr')^{|l|}\right] , \tag{84}$$

where $r_< = \min(r,r')$ and $r_> = \max(r,r')$. This identity is a simple corollary of Eqs. (13) and (14). Thus

$$F_l(r_m,r_{m'}) = \frac{1}{2lr_m}\left\{A_l(r_{m'})\left[\left(\frac{\min(r_m,r_{m'})}{\max(r_m,r_{m'})}\right)^l - (r_m r_{m'})^l\right] + \int_{r_{m'}}^1 dr'\, B_l(r')\left[\left(\frac{\min(r_m,r')}{\max(r_m,r')}\right)^l - (r_m r')^l\right]\right\} . \tag{85}$$

For the special case $m = m'$, we have

$$F_l(r_m,r_m) = \frac{1}{2lr_m}\left[A_l(r_m)(1-r_m^{2l}) + r_m^l\int_{r_m}^1 dr\, B_l(r)(r^{-l}-r^l)\right] , \tag{86}$$

which is used in Eq. (82).

VI Conclusion

We have developed a general, two-dimensional theory for analyzing shear Alfvén wave problems in toroidal geometry. Instead of using the usual poloidal harmonics, we expand the

wave function in the natural basis provided by the eigenfunctions of the toroidal Alfvén continuum, which allows us to reduce the system to a few integral equations valid for arbitrary mode numbers n. These basis functions themselves embody the essential aspects of the shear Alfvén physics. They are the solution of an ODE, so analytic expressions can often be found. It is important to note that the ODE description of toroidal Alfvén continuum rests solely upon the assumption of axisymmetry. Accurate analytic expressions for the continuum eigenfunctions and the associated eigenvalues, combined with the small number of the reduced equations, makes this new approach very powerful for practical calculations. Moreover, the integral equations of the reduced system have the same structure as the Vlasov equation, so there is a rich source of materials that we can tap to further our search for solutions of the toroidal Alfvén wave problems.

In this paper we have considered the standard TAE model. We have shown that the new method leads to analytic expressions for the dispersion relation, for the eigenfunctions of the discrete TAE modes, and also for the eigenfunctions of the continuum TAE modes. We have also demonstrated that, unless all the gaps line up with each other, the TAE spectrum is purely continuous. Our results are valid for arbitrary mode numbers n and inverse aspect ratio $\hat{\epsilon}$, even though the model equation we use is derived for small $\hat{\epsilon}$. The dispersion relation is expressed in terms of Cauchy-type integrals, which makes it possible to study its analytic continuation by choosing the appropriate Landau contours. We have found that the dispersion function is multivalued with many overlapping branch cuts, signaling the extreme complexity of its Riemann surface. A thorough analysis of the Riemann surface structure of the dispersion function is necessary for a complete understanding of the TAE continuum damping (within the MHD framework). Such a study may be the subject of future research.

In the vanishing $\hat{\epsilon}$ limit, we have shown that the integral equations are further reduced to a recurrence relation. The coefficients in this recurrence relation are all given explicitly, in contrast to some of the previous works based on boundary layer analysis. For the case

of a single gap, we have obtained an explicit expression for the eigenfrequency and found it in agreement with the previously known result. Once the eigenfrequency is found, we can write immediately the explicit analytic expression for the two-dimensional mode structure.

Acknowledgments

The authors would like to thank G.Y. Fu, C.T. Hsu, D.J. Sigmar, X.D. Zhang, and Y.Z. Zhang for stimulating discussions. This work was supported by the US Department of Energy Contract No. DE-FG05-80ET-53088.

Appendix A: The Green's Function for $\nabla_\perp{}^2$

This appendix contains a derivation of the Green's function (12) for the two-dimensional Laplacian. We will calculate it in two different ways in order to establish both Eqs. (13) and (14). Some of the materials presented here can be found in Ref. 38.

In the polar coordinates the Green's function satisfies the following equation:

$$\left[\frac{1}{r}\frac{\partial}{\partial r}r\frac{\partial}{\partial r}+\frac{1}{r^2}\frac{\partial^2}{\partial\theta^2}\right]G(r,\theta;r',\theta')=\frac{1}{r}\delta(r-r')\delta(\theta-\theta')\ . \tag{A.1}$$

The boundary conditions require G to be periodic in both θ and θ', to be finite at $r,r'=0$, and to vanish at $r,r'=1$. Clearly G depends only on the difference $\theta-\theta'$, so it can be expanded into a Fourier series:

$$G(r,\theta;r',\theta')=\sum_l G_l(r,r')e^{il(\theta-\theta')}\ . \tag{A.2}$$

Substituting it into Eq. (A.1) we obtain

$$\left[\frac{1}{r}\frac{\partial}{\partial r}r\frac{\partial}{\partial r}-\frac{l^2}{r^2}\right]G_l(r,r')=\frac{1}{2\pi r}\delta(r-r')\ . \tag{A.3}$$

This equation can be solved using two different methods. In the first method we analyze the eigenvalue problem for the operator on the left-hand side of Eq. (A.3):

$$\left[\frac{1}{r}\frac{d}{dr}r\frac{d}{dr}-\frac{l^2}{r^2}\right]e_l=-k_\perp^2 e_l\ . \tag{A.4}$$

The general solution of this equation can be expressed as a linear combination of Bessel functions $J_l(k_\perp r)$ and $Y_l(k_\perp r)$. The boundary condition at $r=0$ excludes all $Y_l(k_\perp r)$, while the boundary condition at $r=1$ requires $J_l(k_\perp)=0$, yielding $k_\perp=\xi_{lk}$, with ξ_{lk} as the kth zero of $J_l(x)$. Since the functions $J_l(\xi_{lk}r)$ for $k=0,1,2,\ldots$ form an orthogonal and complete set, with the orthogonality condition[38]

$$\int_0^1 dr\, r J_l(\xi_{lk}r)J_l(\xi_{lk'}r)=\frac{1}{2}J_{l+1}^2(\xi_{lk})\,\delta_{k,k'}\ , \tag{A.5}$$

we can expand $G_l(r,r')$ in terms of $J_l(\xi_{lk}r)$:

$$G_l(r,r') = \sum_k a_{lk}(r') J_l(\xi_{lk} r) \ . \tag{A.6}$$

Using this in Eq. (A.3), and applying the orthogonality condition (A.5), we obtain

$$a_{lk}(r') = -\frac{J_l(\xi_{lk} r')}{2\pi N_{lk}^2} \ , \tag{A.7}$$

where N_{lk} is given by Eq. (15). Substituting it into Eq. (A.6), we then arrived at Eq. (13), the first representation for $G_l(r,r')$.

The second method of solving Eq. (A.3) considers the homogeneous equation for the two regions $r < r'$ and $r > r'$ separately, then match the solutions at $r = r'$. For $l \neq 0$, the two linearly independent solutions are $r^{\pm l}$. Taking into account of the boundary conditions at $r = 0$ and 1 we have

$$G_l(r,r') = \begin{cases} A(r') r^{|l|} \ , & \text{if } r < r' \ ; \\ B(r')(r^{|l|} - r^{-|l|}) \ , & \text{if } r > r' \ . \end{cases} \tag{A.8}$$

From Eq. (A.3) we find the matching conditions to be

$$\begin{aligned} \lim_{\delta \to +0} [G_l(r' + \delta, r') - G_l(r' - \delta, r')] = 0 \ , \\ \lim_{\delta \to +0} [\partial_r G_l(r' + \delta, r') - \partial_r G_l(r' - \delta, r')] = \tfrac{1}{2\pi r'} \ . \end{aligned} \tag{A.9}$$

Substituting Eq. (A.8)into (A.9) and then solving for A and B, we obtain

$$\begin{aligned} A(r') = (r'^{|l|} - r'^{-|l|})/4\pi|l| \ , \\ B(r') = r'^{|l|}/4\pi|l| \ . \end{aligned} \tag{A.10}$$

Inserting this into Eq. (A.8) we finally obtain a concise expression for G_l:

$$G_l(r,r') = \frac{1}{4\pi|l|} \left[(rr')^{|l|} - \left(\frac{r_<}{r_>} \right)^{|l|} \right] \ , \tag{A.11}$$

where $r_< \equiv \min(r,r')$, and $r_> \equiv \max(r,r')$. The result for $l = 0$ can be derived in a similar manner, and the result is

$$G_0(r,r') = \frac{1}{2\pi} \ln r_> \ . \tag{A.12}$$

Thus we have proved Eq. (14), the second representation for $G_l(r,r')$.

Appendix B: Continuum Eigenvalues and Eigenfunctions

In this appendix we calculate the eigenvalues and eigenfunctions of the toroidalAlfvéncontinuum in the limit of small $\hat{\epsilon}$.

The eigenvalues λ_i of the Mathieu equation are to be calculated from Eq. (30). For small values of b, the Hill's determinant $\Delta(\lambda, b)$ can be expanded to order b^2, yielding an approximate eigenvalue equation:[35]

$$\cos \pi\nu = \cos \pi\sqrt{\lambda} + \frac{\pi b^2}{4} \frac{\sin \pi\sqrt{\lambda}}{\sqrt{\lambda}(\lambda - 1)} + \mathcal{O}(b^4) \ . \tag{B.1}$$

We shall see in a moment that this approximation gives eigenvalues accurate to the first order in b, which is adequate for our purpose. From Eq. (32) we have $\lambda \to \nu^2$ as $b \to 0$, so let us expand the right-hand side of Eq. (B.1) into a series of $\lambda - \nu^2$. To the second order we obtain

$$A(\nu)\,(\lambda - \nu^2)^2 + B(\nu)\,(\lambda - \nu^2) + C(\nu) = 0 \ , \tag{B.2}$$

where

$$A(\nu) = -\frac{\pi}{8}\left[\frac{\pi\nu \cos \pi\nu - \sin \pi\nu}{\nu^3}\right] + \mathcal{O}(b^2) \ , \tag{B.3}$$

$$B(\nu) = -\frac{\pi \sin \pi\nu}{2\nu} + \frac{\pi b^2}{8}\left[\frac{(\nu^2 - 1)(\pi\nu \cos \pi\nu - \sin \pi\nu) - 2\nu^2 \sin \pi\nu}{\nu^3(\nu^2 - 1)^2}\right] + \mathcal{O}(b^4) \ , \tag{B.4}$$

$$C(\nu) = \frac{\pi b^2}{4} \frac{\sin \pi\nu}{\nu(\nu^2 - 1)} + \mathcal{O}(b^4) \ . \tag{B.5}$$

The discriminant of this quadratic equation is remarkably simple:

$$B^2 - 4AC = \frac{\pi^2 \sin^2 \pi\nu}{4\nu^2(\nu^2 - 1)^2}\left[(\nu^2 - 1)^2 + b^2\right] + \mathcal{O}(b^4) \ . \tag{B.6}$$

Thus the solutions of Eq. (B.2) are

$$\lambda - \nu^2 = \frac{2C}{-B \pm \sqrt{B^2 - 4AC}}$$

$$= \frac{\frac{\pi b^2 \sin \pi\nu}{2\nu(\nu^2-1)}}{\frac{\pi \sin \pi\nu}{2\nu} \pm \sqrt{\frac{\pi^2 \sin^2 \pi\nu}{4\nu^2(\nu^2-1)^2}\left[(\nu^2-1)^2+b^2\right]}} + \mathcal{O}(b^2) \tag{B.7}$$

$$= -(\nu^2-1) \pm \sqrt{(\nu^2-1)^2+b^2} + \mathcal{O}(b^2) \ .$$

Notice that the accuracy of this result changes as ν varies: the error is $\mathcal{O}(b^4)$ for $|\nu^2-1| \gg b$, but increases to $\mathcal{O}(b^2)$ for $|\nu^2-1| \ll b$, when the two solutions become nearly degenerate. It is important to note that with this accuracy we can only resolve the gap structure between the lowest two eigenvalues $\lambda_0(r)$ and $\lambda_1(r)$. The choice of signs for the two eigenvalues can be determined by inspection. Denoting $s_0 = -1$, $s_1 = 1$, we have, for $i = 0$ and 1,

$$\lambda_i(r) \approx 1 + s_i\sqrt{(\nu_i^2-1)^2+b^2} \ . \tag{B.8}$$

From Eq. (34) we find the continuum eigenvalue $\sigma_i(r,\omega)$:

$$\sigma_i(r,\omega) = \frac{1}{4q^2}\left[(2q\Omega)^2 - \lambda_i(r)\right] \ . \tag{B.9}$$

Setting $\sigma_i(r,\omega) = 0$ we can explicitly solve for the continuum eigenfrequency $\omega_i(r)$. The result is

$$\omega_i^2(r) = \left(\frac{v_A}{2qR_0}\right)^2 \frac{1 + s_i\sqrt{(\nu_i^2-1)^2 + \widehat{\epsilon}^2\nu_i^2(2-\nu_i^2)}}{1-\widehat{\epsilon}^2} \ . \tag{B.10}$$

The curves in Fig. 2 are plotted using these formulas.

Now that we know $\lambda_i(r)$, we can calculate the continuum eigenfunctions using the recurrance relation (29). In the small b limit, we can neglect all u_l^i for $|l| \geq 2$. Then from Eq. (29) we obtain

$$\frac{u_{\pm 1}^i}{u_0^i} \approx \frac{b}{\lambda_i - (\nu_i \pm 2)^2} \ . \tag{B.11}$$

This equation indicates that, away from the gaps, we have $u_{\pm 1}^i = \mathcal{O}(b)$, which is also negligible. In the vicinity of a gap, where $|\nu_i| \approx 1$, one of the $u_{\pm 1}^i$ components can become comparable to u_0^i (which one depends on the sign of ν_i. As pointed out in Sec. III, ν_i

changes sign at the gaps.) Figure 3 summarizes graphically the values of the functions $m_i(r)$ and $\nu_i(r)$ near the gap m whose radial location is determined by Eq. (70). Also shown are the significant components of u_l^i, which we shall discuss below.

First we observe that, for frequencies in the gap region, $(2q\Omega)^2 \approx 1$. It is therefore convenient to introduce a function g_m to represent the relative displacement of frequency from the center of gap m, defined by $g_m \equiv [(2q_m\Omega)^2 - 1]/\widehat{\epsilon}_m$, where $\widehat{\epsilon}_m \equiv \widehat{\epsilon}(r_m)$. In what follows we denote $x \equiv r - r_m$, and keep only the radial variation of $\nu_i(r)$; thus we have $b \approx -\widehat{\epsilon}_m$.

Now consider the continuum with $i = 0$. To the left of the gap, where $x < 0$, we have $m_0(r) = m$, so from Eq. (33) we find

$$\nu_0(r) = 2(m - nq) \approx -1 - 2nq'_m x \ , \tag{B.12}$$

Substituting it into Eq. (B.8) we obtain

$$\lambda_0(r) \approx 1 - \sqrt{(4nq'_m x)^2 + \epsilon_m^2} \ . \tag{B.13}$$

Then from Eq. (B.9) we have

$$\sigma_0(r,\omega) \approx \frac{1}{4q_m^2}\left[\widehat{\epsilon}_m g_m + \sqrt{(4nq'_m x)^2 + \epsilon_m^2}\right] \ . \tag{B.14}$$

Substituting Eqs. (B.12) and (B.13) into Eq. (B.11) we find

$$\frac{u_{-1}^0}{u_0^0} = \mathcal{O}(\widehat{\epsilon}) \ , \qquad \frac{u_1^0}{u_0^0} \approx \eta_0 \ , \tag{B.15}$$

where

$$\eta_0(r) \equiv \frac{\widehat{\epsilon}_m}{\sqrt{(4nq'_m x)^2 + \epsilon_m^2} + |4nq'_m x|} \ . \tag{B.16}$$

Thus the ratio u_1^0/u_0^0 approaches 1 as $x \to 0$.

To the right of the gap, where $x > 0$, we have $m_0(r) = m + 1$, so

$$\nu_0(r) = 2(m + 1 - nq) \approx 1 - 2nq'_m x \ . \tag{B.17}$$

It has been pointed out in Sec. III that $\lambda_i(r)$ and $\sigma_i(r,\omega)$ vary continuously across a gap, so Eqs. (B.13) and (B.14) remain valid for this region. One can also see this fact by noting that λ_0 and σ_0 are even in x. Using Eqs. (B.13) and (B.17) we find

$$\frac{u^0_{-1}}{u^0_0} \approx \eta_0 \ , \qquad \frac{u^0_1}{u^0_0} = \mathcal{O}(\widehat{\epsilon}) \ . \tag{B.18}$$

For the continuum with $i = 1$, the calculations are similar. For $x < 0$, we have $m_1(r) = m + 1$, and $\nu_1(r) \approx 1 - 2nq'_m x$. From Eqs. (B.8) and (B.9) we have

$$\lambda_1(r) \approx 1 + \sqrt{(4nq'_m x)^2 + \epsilon_m^2} \ , \tag{B.19}$$

$$\sigma_1(r,\omega) \approx \frac{1}{4q_m^2}\left[\widehat{\epsilon}_m g_m - \sqrt{(4nq'_m x)^2 + \epsilon_m^2}\right] \ , \tag{B.20}$$

which are also valid for $x > 0$. Similarly Eq. (B.11) yields

$$\frac{u^1_{-1}}{u^1_0} \approx -\eta_1 \ , \qquad \frac{u^1_1}{u^1_0} = \mathcal{O}(\widehat{\epsilon}) \ , \tag{B.21}$$

where

$$\eta_1(r) \equiv \frac{\widehat{\epsilon}_m}{\sqrt{(4nq'_m x)^2 + \epsilon_m^2} - |4nq'_m x|} \ . \tag{B.22}$$

For $x > 0$, we have $m_1(r) = m$, implying $\nu_1(r) \approx -1 - 2nq'_m x$, and

$$\frac{u^1_{-1}}{u^1_0} = \mathcal{O}(\widehat{\epsilon}) \ , \qquad \frac{u^1_1}{u^1_0} \approx -\eta_1 \ . \tag{B.23}$$

The principal results of this appendix are contained in Eqs. (B.15), (B.18), (B.21), and (B.23). From these we obtain the following Fourier coefficients for the continuum eigenfunctions: For $x < 0$,

$$\begin{aligned} u^0_l(r) &\approx \delta_{l,0} + \eta_0(r)\delta_{l,1} \ , \\ u^1_l(r) &\approx \delta_{l,0} - \eta_1(r)\delta_{l,-1} \ ; \end{aligned} \tag{B.24}$$

for $x > 0$,

$$\begin{aligned} u^0_l(r) &\approx \delta_{l,0} + \eta_0(r)\delta_{l,-1} \ , \\ u^1_l(r) &\approx -[\delta_{l,0} - \eta_1(r)\delta_{l,1}] \ . \end{aligned} \tag{B.25}$$

Here we have chosen the normalization factor so that the continuum eigenfunctions $\psi_j(r,\theta)$ [Eq. (35) are continuous across the gap.

Appendix C: Calculation of $H_{ll'}(r_m)$

In this appendix we use the results obtained in Appendix B to calculate the functions $H_{ll'}(r_m)$ as defined in Eq. (71). From Eqs. (B.24) and (B.25) we have, for $x < 0$,

$$\begin{aligned} u^0_{l-m_0} &= \delta_{l,m} + \eta_0 \delta_{l,m+1} \ , \\ u^1_{l-m_1} &= \delta_{l,m+1} - \eta_1 \delta_{l,m} \ ; \end{aligned} \tag{C.1}$$

and for $x > 0$,

$$\begin{aligned} u^0_{l-m_0} &= \delta_{l,m+1} + \eta_0 \delta_{l,m} \ , \\ u^1_{l-m_1} &= -(\delta_{l,m} - \eta_1 \delta_{l,m+1}) \ . \end{aligned} \tag{C.2}$$

Substituting these into Eq. (71) we obtain

$$H_{ll'}(r_m) = \int_{-\infty}^{0} dx \left[\frac{(\delta_{l,m} + \eta_0 \delta_{l,m+1})(\delta_{l',m} + \eta_0 \delta_{l',m+1})}{(1+\eta_0^2)\sigma_0(r_m + x, \omega)} + \frac{(\delta_{l,m+1} - \eta_1 \delta_{l,m})(\delta_{l',m+1} - \eta_1 \delta_{l',m})}{(1+\eta_1^2)\sigma_1(r_m + x, \omega)} \right]$$

$$+ \int_{0}^{-\infty} dx \left[\frac{(\delta_{l,m+1} + \eta_0 \delta_{l,m})(\delta_{l',m+1} + \eta_0 \delta_{l',m})}{(1+\eta_0^2)\sigma_0(r_m + x, \omega)} + \frac{(\delta_{l,m} - \eta_1 \delta_{l,m+1})(\delta_{l',m} - \eta_1 \delta_{l',m+1})}{(1+\eta_1^2)\sigma_1(r_m + x, \omega)} \right] . \tag{C.3}$$

Since the functions η_i and σ_i are even in x, we can extend the limits of both integrals to $\pm\infty$ and divide the result by 2. Straightforward algebra shows that $H_{ll'}(r_m)$ is tridiagonal:

$$H_{ll'}(r_m) = \alpha_m(\delta_{l,m}\delta_{l',m} + \delta_{l,m+1}\delta_{l',m+1}) + \beta_m(\delta_{l,m+1}\delta_{l',m} + \delta_{l,m}\delta_{l',m+1}) \ , \tag{C.4}$$

where α_m and β_m are functions of frequency, defined by

$$\alpha_m \equiv \frac{1}{2} \int_{-\infty}^{+\infty} dx \left[\frac{1}{\sigma_0} + \frac{1}{\sigma_1} \right] \ , \tag{C.5}$$

$$\beta_m \equiv \int_{-\infty}^{+\infty} dx \left[\frac{\eta_0}{1+\eta_0^2} \frac{1}{\sigma_0} - \frac{\eta_1}{1+\eta_1^2} \frac{1}{\sigma_1} \right] \ , \tag{C.6}$$

Using Eqs. (B.14), (B.16), (B.22), and (B.20) we find, after some algebra, the following simple formulas:

$$\alpha_m = \frac{\pi q_m^2}{n q_m'} \frac{-g_m}{\sqrt{1-g_m^2}} \ , \qquad \beta_m = \frac{\pi q_m^2}{n q_m'} \frac{1}{\sqrt{1-g_m^2}} \ . \tag{C.7}$$

These results are used in Sec. V.

References

1. D.W. Ross, G.L. Chen, and S.M. Mahajan, Phys. Fluids **25**, 652 (1982).

2. K. Appert, R. Gruber, F. Troyon, and J. Vaclavik, Plasma Phys. **24**, 1147 (1982).

3. S.M. Mahajan, D.W. Ross, and G.L. Chen, Phys. Fluids **26**, 2195 (1983).

4. S.M. Mahajan, Phys. Fluids **27**, 2238 (1984).

5. S. Riyopoulos and S.M. Mahajan, Phys. Fluids **29**, 737 (1986).

6. C.Z. Cheng and M.S. Chance, Phys. Fluids **29**, 3695 (1986).

7. C.Z. Cheng, L. Chen, and M.S. Chance, Ann. Phys. **161**, 21 (1985).

8. C.Z. Cheng and M.S. Chance, J. Comput. Phys. **71**, 124 (1987).

9. G.Y. Fu and J.W. Van Dam, Phys. Fluids B **1**, 1949 (1989)

10. K.L. Wong, Phys. Rev. Lett. **66**, 1874 (1991).

11. W.W. Heidbrink, E.J. Strait, E. Doyle, and R. Snider, Nucl. Fusion **31**, 1635 (1991).

12. R.R. Mett and S.M. Mahajan, Phys. Fluids B **4**, 2885 (1992).

13. F. Zonca and L. Chen, Phys. Rev. Lett. **68**, 592 (1992).

14. M.N. Rosenbluth, H.L. Berk, J.W. Van Dam, and D.M. Lindberg, Phys. Rev. Lett. **68**, 596 (1992).

15. M.N. Rosenbluth, H.L. Berk, J.W. Van Dam, and D.M. Lindberg, Phys. Fluids B **4**, 2189 (1992).

16. H.L. Berk, J.W. Van Dam, Z. Guo, and D.M. Lindberg, Phys. Fluids B **4**, 1806 (1992).

17. Z. Sedlacek, Czech. J. Phys. B **22**, 439 (1972).

18. Z. Sedlacek, Czech. J. Phys. B **23**, 892 (1973).

19. Z. Sedlacek, J. Plasma Phys. **5**, 239 (1971).

20. Z. Sedlacek, J. Plasma Phys. **6**, 187 (1971).

21. Z. Sedlacek and B. Roberts, J. Plasma Phys. **41**, 97 (1989).

22. C. Uberoi, Phys. Fluids **15**, 1673 (1972).

23. C. Uberoi and Z. Sedlacek, Phys. Fluids B **4**, 6 (1992).

24. J.D. Crawford and P.D. Hislop, Ann. Phys. **189**, 265 (1989).

25. Z. Sedlacek and L. Nocera, to appear in J. Plasma Phys. **48**, (1992).

26. J. Larsson, Phys. Rev. Lett. **66**, 1466 (1991).

27. P.J. Morrison and D. Pfirsch, to appear in Phys. Fluids B (1992).

28. Y.P. Pao, Nucl. Fusion **15**, 631 (1975).

29. J.P. Goedbloed, Phys. Fluids **18**, 1258 (1975).

30. J.A. Tataronis, J.N. Talmadge, and J.L. Shohet, in *Proc. of 3rd Topical Conference on Radio Frequency Plasma Heating, Pasadena,1978.*

31. E. Hameiri and J. H. Hammer, Phys. Fluids **22**, 1700 (1979).

32. O.P. Pogutse and E.I. Yurchenko, Nucl. Fusion **18**, 1629 (1978).

33. D.A. D'Ippolito and J.P. Goedbloed, Plasma Phys. **22**, 1091 (1980).

34. C.E. Kieras and J.A. Tataronis, J. Plasma Phys. **28**, 395 (1982).

35. N.W. McLachlan, *Theory and Application of Mathieu Functions* (Dover, New York, 1964).

36. F.D. Gakhov, *Boundary Value Problems* (Addison-Wesley, Reading, Mass., 1966).

37. G.Y. Fu, private communications.

38. P.M. Morse and H. Feshbach, *Methods of Theoretical Physics* (McGraw-Hill, New York, 1953).

Figure Captions

1. A stability diagram for the Mathieu equation. The shaded regions are the forbidden zones where the eigenfunction is unbounded, and the unshaded regions are the allowed zones where the eigenfunction has the Floquet form. The dashed lines depicts how the parameters typically change as r increases.

2. A schematic diagram for the toroidal Alfvén continuum. Only the lowest two continua are plotted. The vertical dashed lines indicate the radial location of the gaps.

3. This diagram summarizes the behavior of various functions in the vicinity of gap m. The functions $m_j(r)$, $\nu_j(r)$, and the Fourier coefficients for the continuum eigenfunction $u_l^j(r)$ are displayed. Detailed calculations are given in Appendix B.

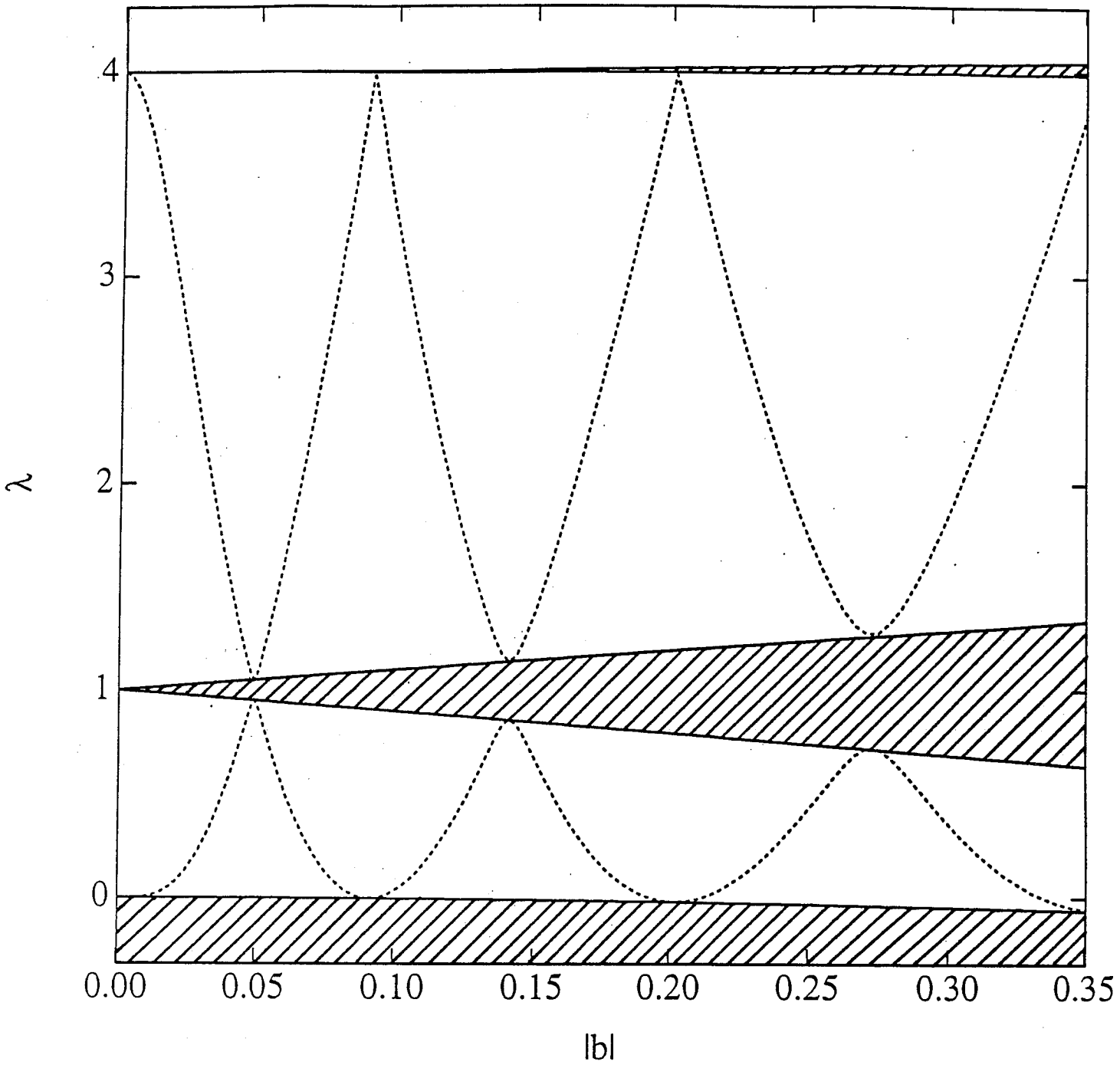

Fig. 1

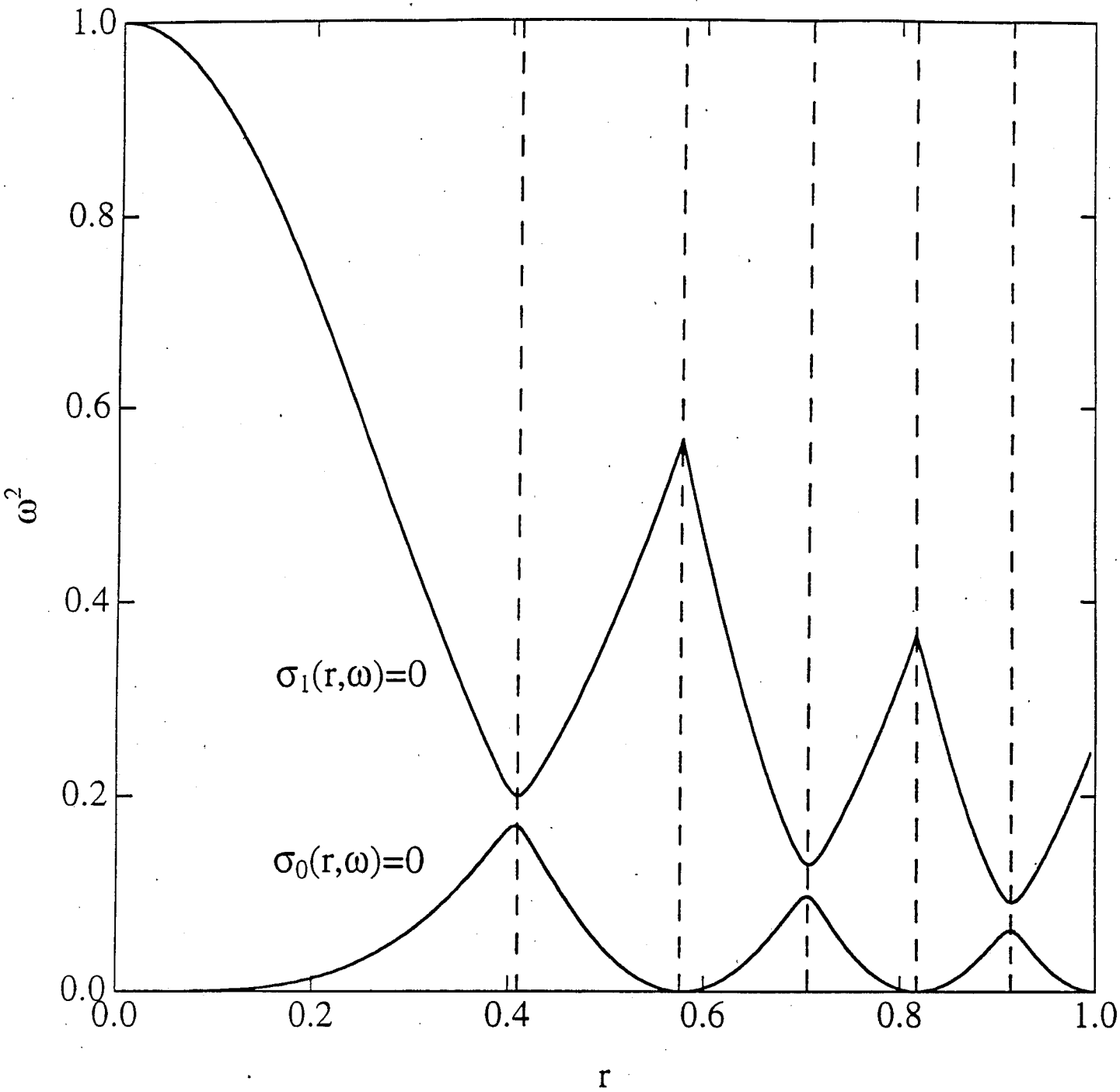
1.0
0.8
0.6
0.4
0.2
0.0
ω^2
$\sigma_1(r,\omega)=0$
$\sigma_0(r,\omega)=0$
0.0
0.2
0.4
0.6
0.8
1.0
r

Fig. 2

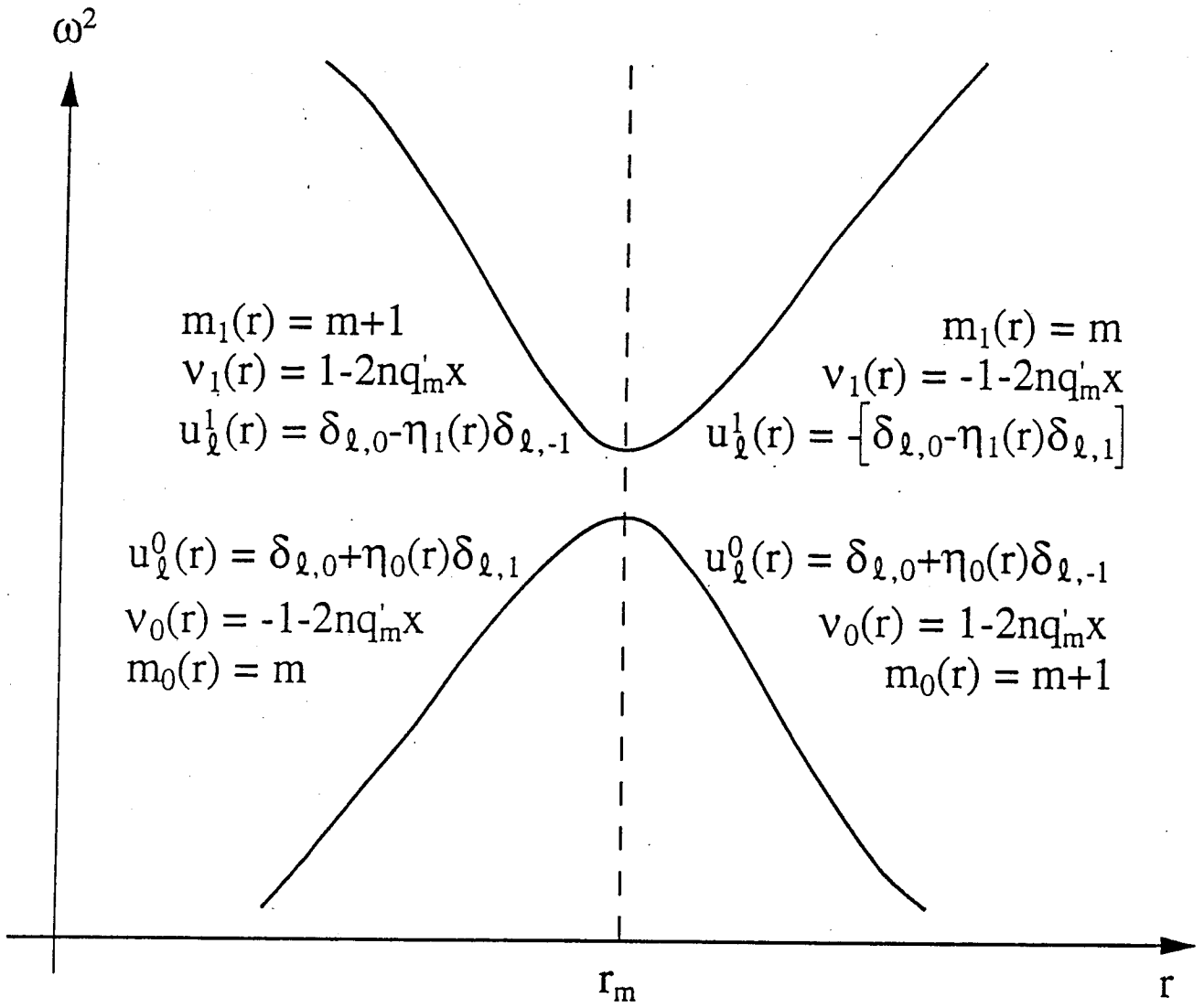
ω^2
$m_1(r) = m+1$
$\nu_1(r) = 1-2nq'_m x$
$u^1_\ell(r) = \delta_{\ell,0}-\eta_1(r)\delta_{\ell,-1}$
$m_1(r) = m$
$\nu_1(r) = -1-2nq'_m x$
$u^1_\ell(r) = -\left[\delta_{\ell,0}-\eta_1(r)\delta_{\ell,1}\right]$
$u^0_\ell(r) = \delta_{\ell,0}+\eta_0(r)\delta_{\ell,1}$
$\nu_0(r) = -1-2nq'_m x$
$m_0(r) = m$
$u^0_\ell(r) = \delta_{\ell,0}+\eta_0(r)\delta_{\ell,-1}$
$\nu_0(r) = 1-2nq'_m x$
$m_0(r) = m+1$
r_m
r

Fig. 3

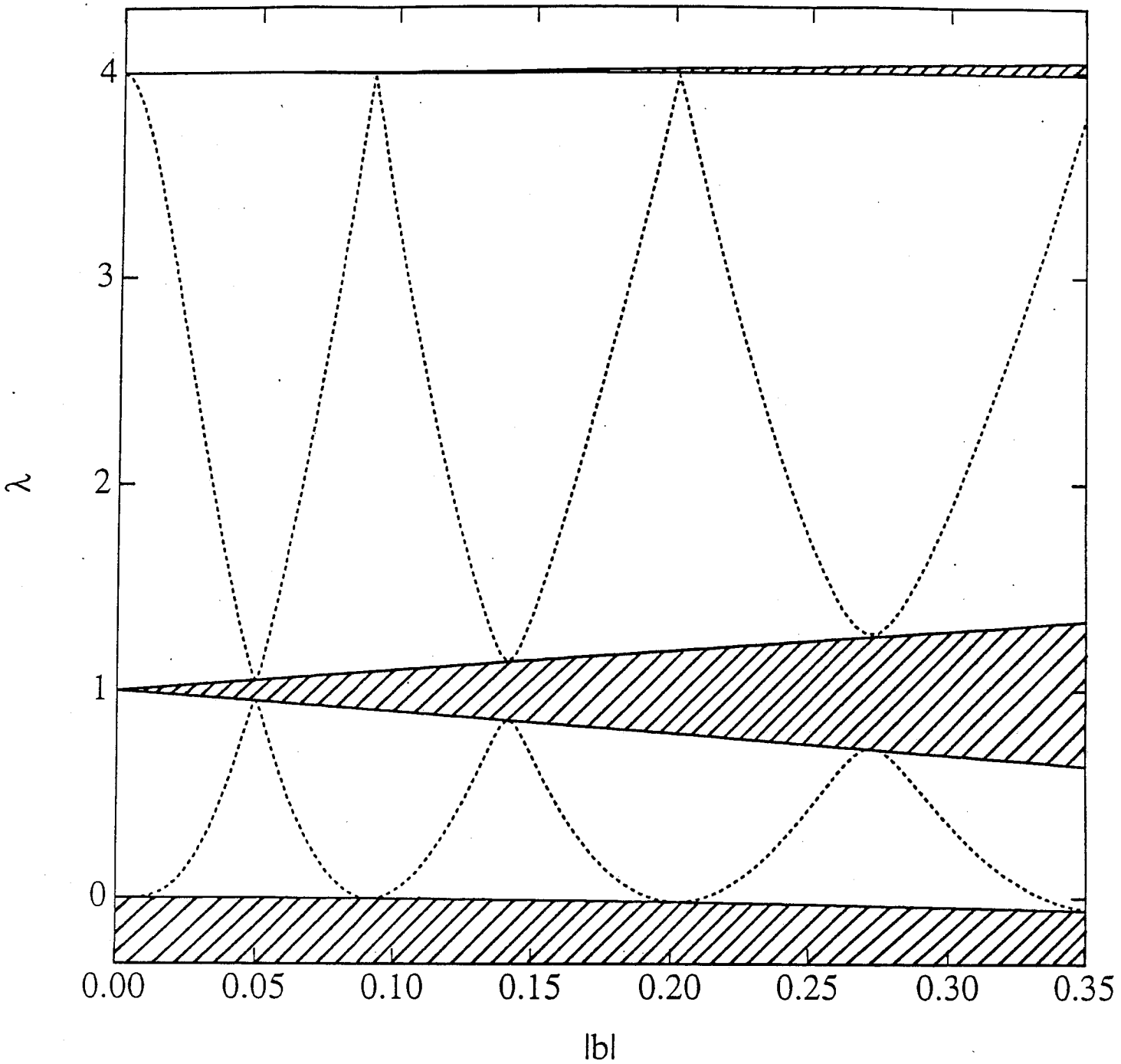
4
3
2
1
0
λ
0.00
0.05
0.10
0.15
0.20
0.25
0.30
0.35
|b|

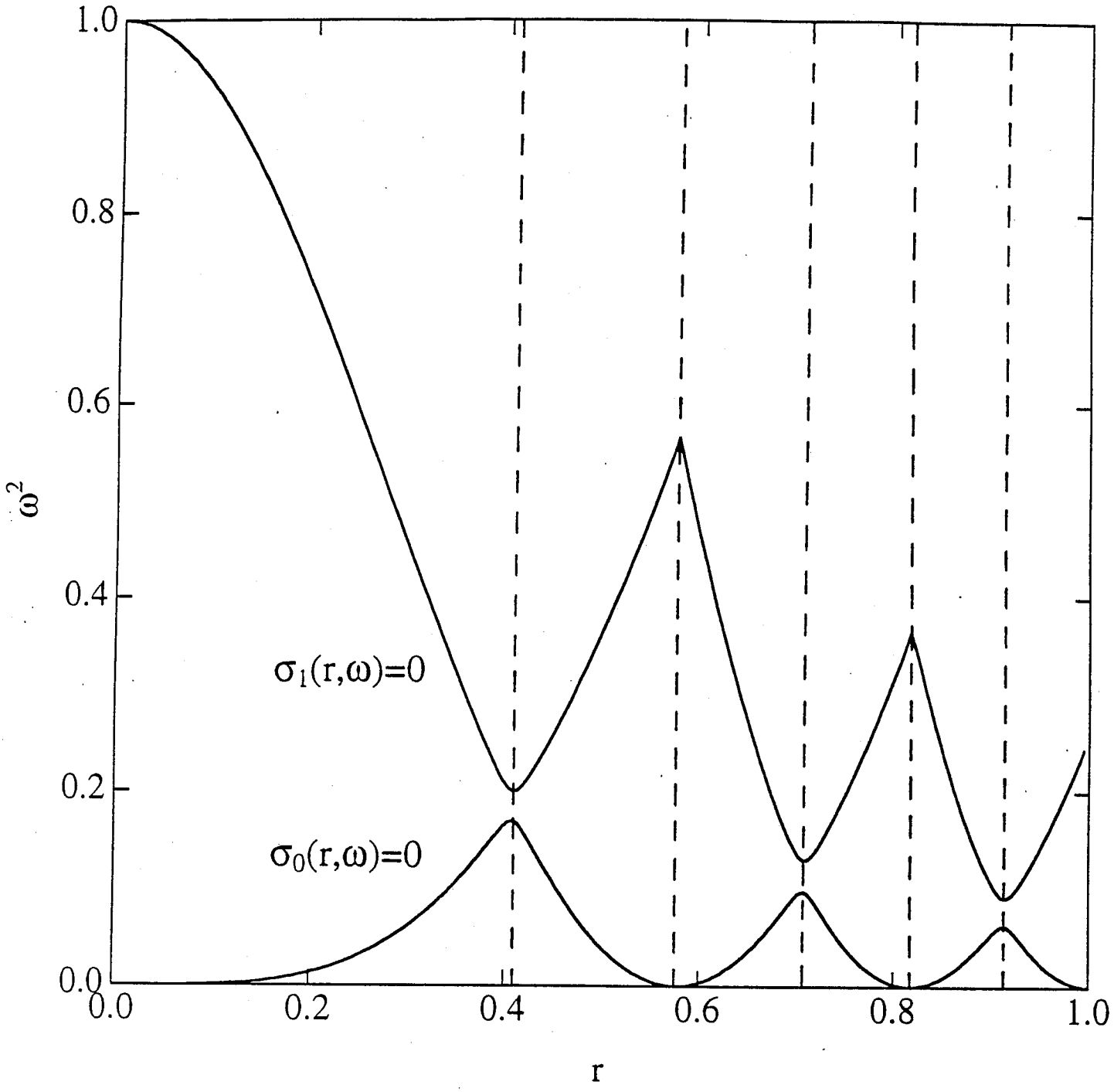
1.0
0.8
0.6
0.4
0.2
0.0
ω^2
$\sigma_1(r,\omega)=0$
$\sigma_0(r,\omega)=0$
0.0
0.2
0.4
0.6
0.8
1.0
r

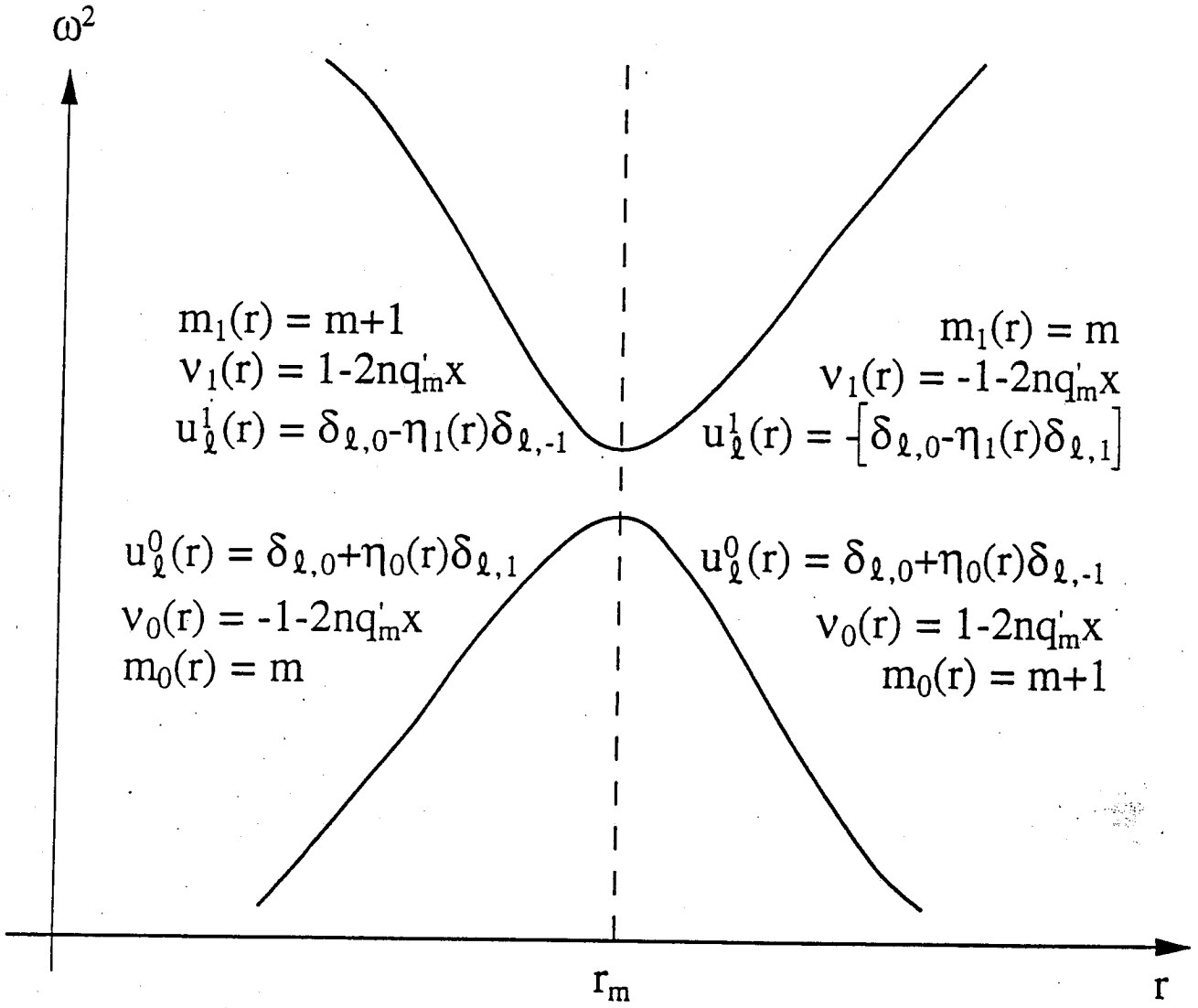
ω^2
$m_1(r) = m+1$
$\nu_1(r) = 1-2nq'_m x$
$u^1_\ell(r) = \delta_{\ell,0}-\eta_1(r)\delta_{\ell,-1}$
$m_1(r) = m$
$\nu_1(r) = -1-2nq'_m x$
$u^1_\ell(r) = -\left[\delta_{\ell,0}-\eta_1(r)\delta_{\ell,1}\right]$
$u^0_\ell(r) = \delta_{\ell,0}+\eta_0(r)\delta_{\ell,1}$
$\nu_0(r) = -1-2nq'_m x$
$m_0(r) = m$
$u^0_\ell(r) = \delta_{\ell,0}+\eta_0(r)\delta_{\ell,-1}$
$\nu_0(r) = 1-2nq'_m x$
$m_0(r) = m+1$
r_m
r

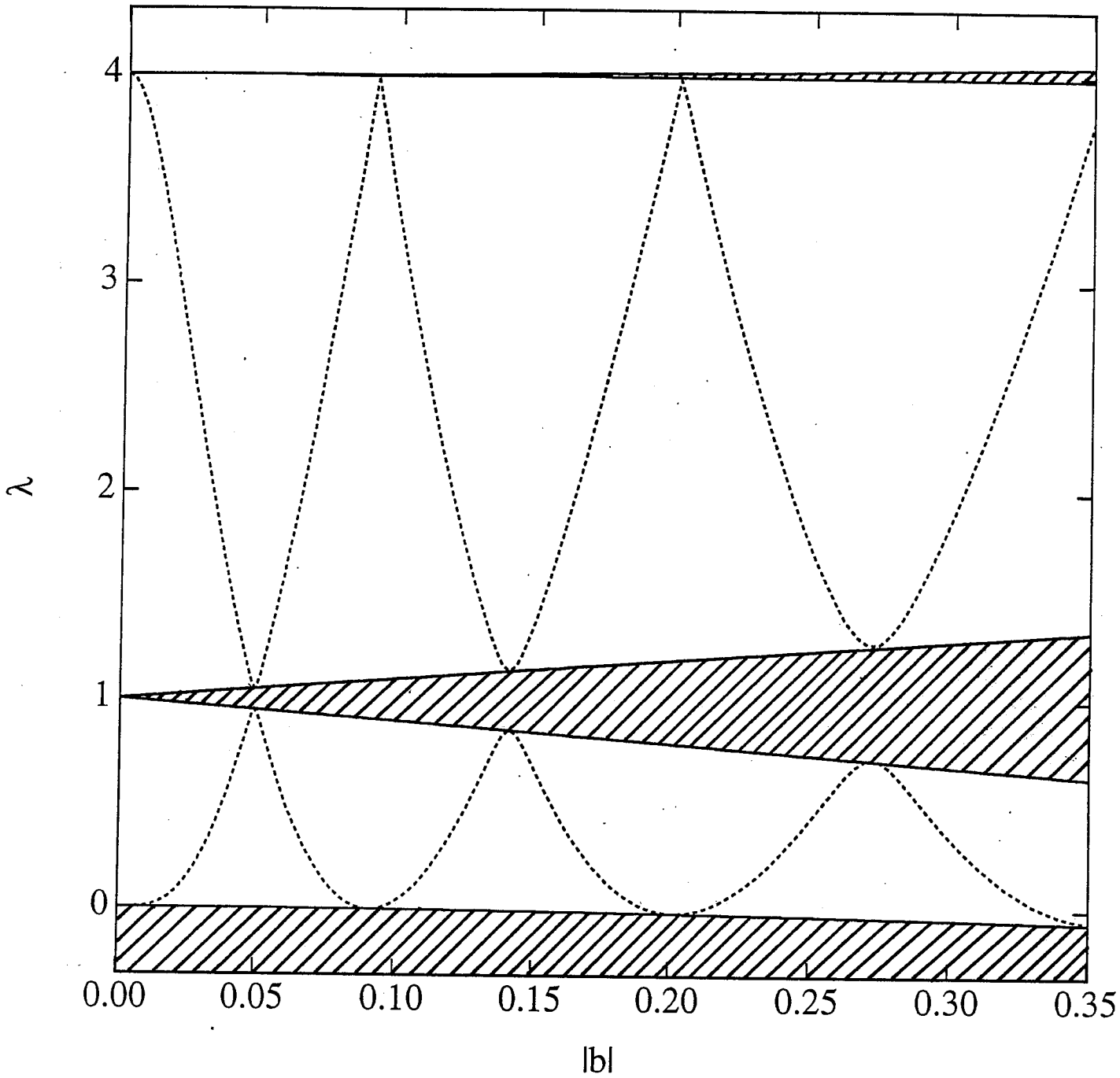

Fig. 1

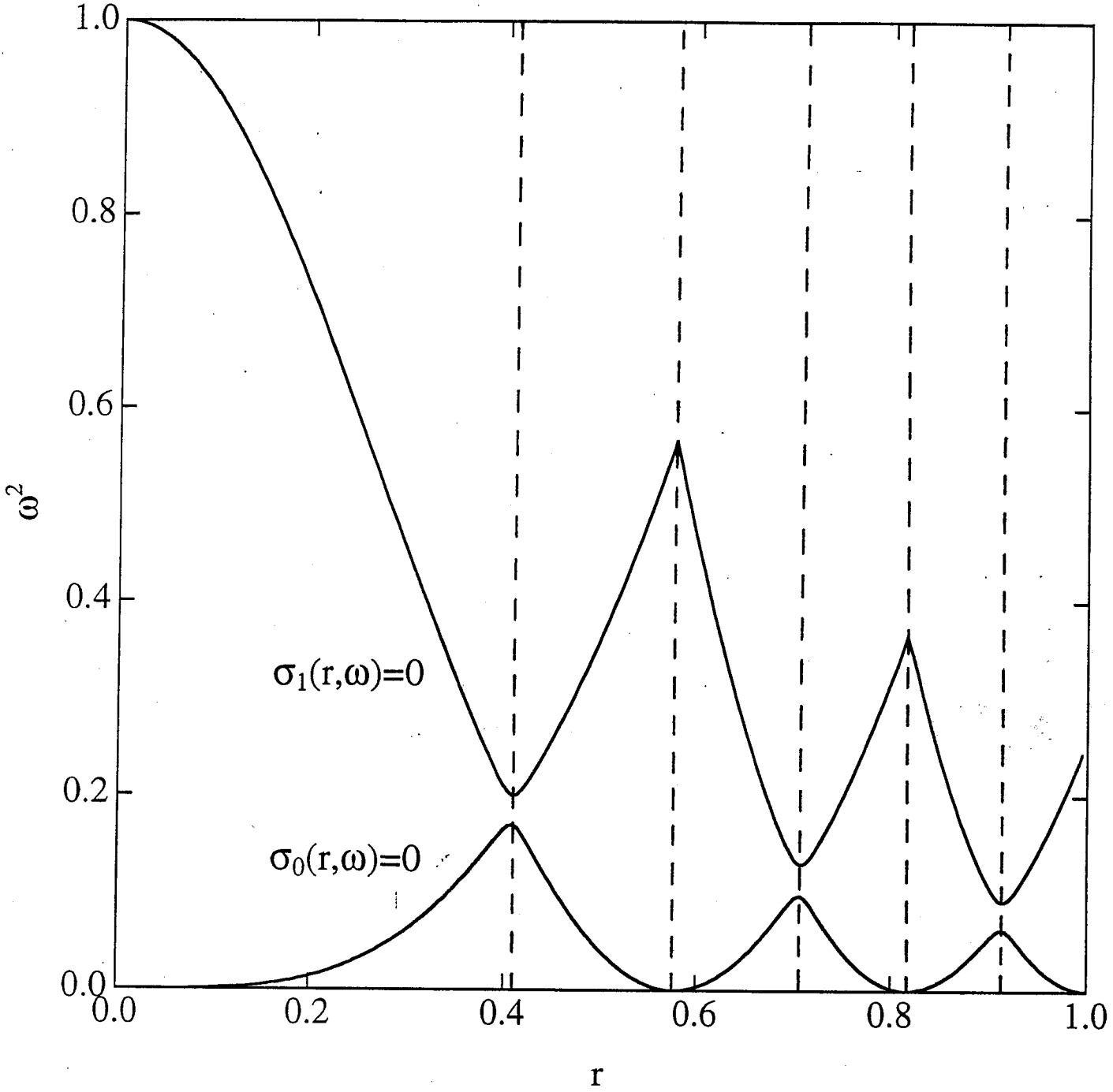
1.0
0.8
0.6
0.4
0.2
0.0
ω^2
$\sigma_1(r,\omega)=0$
$\sigma_0(r,\omega)=0$
0.0
0.2
0.4
0.6
0.8
1.0
r

Fig. 2

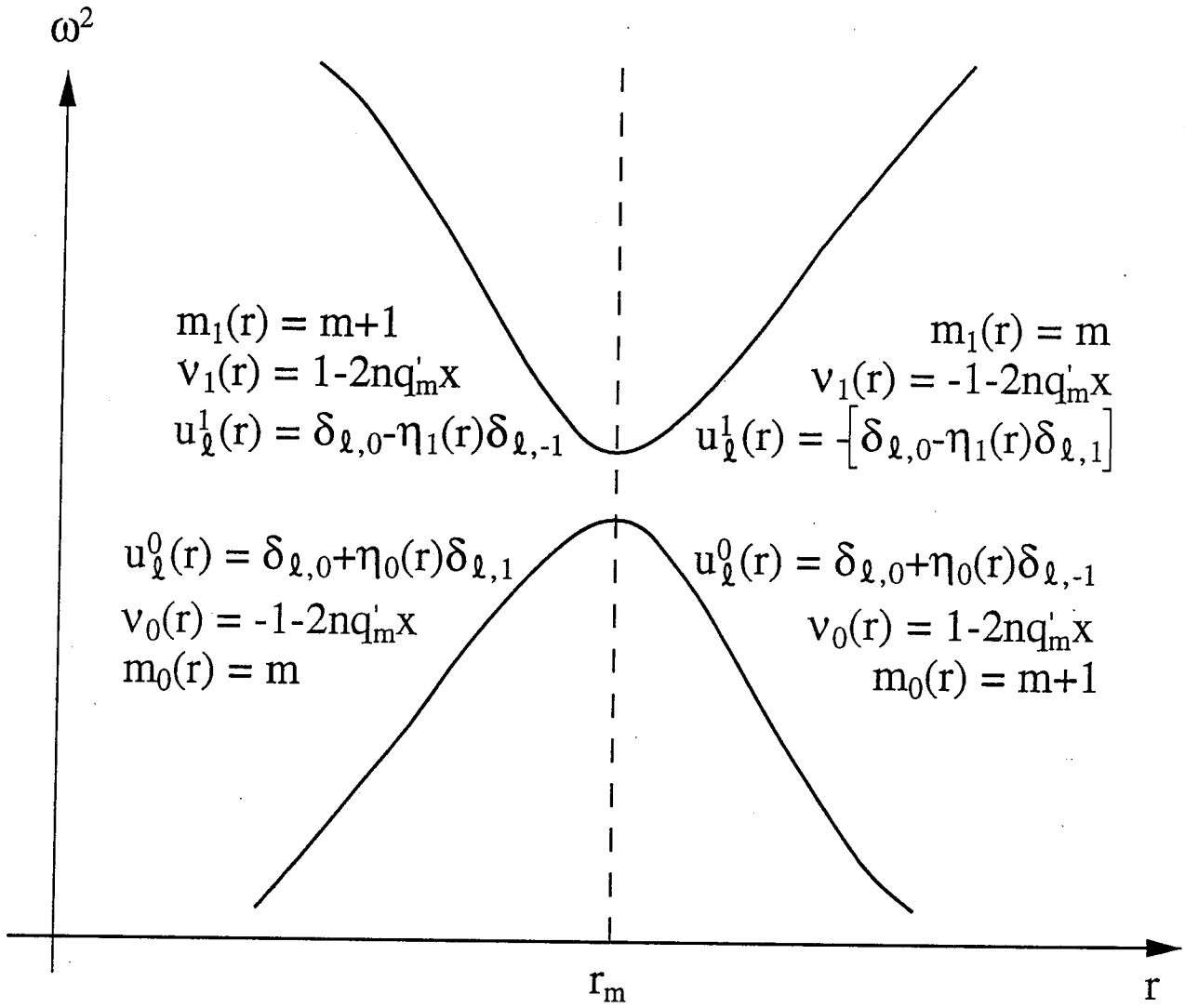
ω^2
$m_1(r) = m+1$
$\nu_1(r) = 1-2nq'_m x$
$u^1_\ell(r) = \delta_{\ell,0}-\eta_1(r)\delta_{\ell,-1}$
$m_1(r) = m$
$\nu_1(r) = -1-2nq'_m x$
$u^1_\ell(r) = -\left[\delta_{\ell,0}-\eta_1(r)\delta_{\ell,1}\right]$
$u^0_\ell(r) = \delta_{\ell,0}+\eta_0(r)\delta_{\ell,1}$
$\nu_0(r) = -1-2nq'_m x$
$m_0(r) = m$
$u^0_\ell(r) = \delta_{\ell,0}+\eta_0(r)\delta_{\ell,-1}$
$\nu_0(r) = 1-2nq'_m x$
$m_0(r) = m+1$
r_m
r

Fig. 3